UNIVERSITÀ DEGLI STUDI DI PADOVA

DIPARTIMENTO DI BIOLOGIA

Corso di Laurea magistrale in Environmental Sustainability and Education

TESI DI LAUREA

Analyzing the function of ERAD in cytokinin signaling and root development in *Arabidopsis thaliana*

Relatore: Prof. Livio Trainotti
Dipartimento di Biologia

Correlatore*: Prof. Tomas Werner
Institute of Biology - University of Graz

Laureanda: Shirin Kordi

ANNO ACCADEMICO 2025/2026

To the pursuit of wisdom, the awakening of awareness, and the hope for a world of peace and freedom.

Acknowledgements

I would like to express my sincere gratitude to my supervisors, Prof. Livio Trainotti and Prof. Tomas Werner, for their invaluable guidance, support, and constructive feedback throughout this work.

I am also deeply grateful to all members of the laboratory for their help, kindness, and support during my time in the lab. I would especially like to thank our laboratory technician, Peter Krbez, for his invaluable technical support and continuous assistance throughout my time in the lab, as well as for his kindness and positive attitude.

I would like to thank the the Erasmus+ Programme, for providing the financial support that made this thesis possible, as well as University of Graz and the University of Padua, for providing the academic framework and the opportunity to carry out this research experience abroad.

Finally, I am deeply grateful to my family, my greatest wealth and deepest source of love, whose encouragement and belief in me have been a constant source of strength. I am especially grateful to my friend Andreas Unterweger for his patience, encouragement, and steadfast support throughout this journey.

Abstract

This study investigated the role of ER-associated degradation (ERAD) components in cytokinin-regulated root development in *Arabidopsis thaliana*, focusing on the E3 ubiquitin ligases *HRD1A, HRD1B, DOA10A, and DOA10B.* Using segregating mutant lines combined with the cytokinin reporter TCSn::GFP, and a CRISPR/Cas9 construct developed for future generation of a doa10a doa10b line, the relationship between ERAD function, cytokinin signaling, and root architecture was examined.

Homozygous ERAD mutant lines were identified through PCR-based genotyping and CAPS marker analysis, confirming the presence of *hrd1 and doa10* loss-of-function alleles in selected lines. Transgenic reporter lines were verified by PCR-based detection of the TCSn::GFP construct.

Root phenotyping revealed that cytokinin (6-benzylaminopurine, BA) strongly inhibited primary root elongation and lateral root formation in a dose-dependent manner across all genotypes. Although minor genotype-dependent differences were observed under control and low cytokinin conditions, cytokinin treatment was the dominant factor shaping root architecture. In particular, doa10a doa10b and the quadruple mutant (*hrd1a hrd1b doa10a doa10b*) showed a visually higher, though not statistically significant, number of lateral roots at low BA concentrations, hinting at a possible modulatory role of ERAD components in cytokinin responsiveness that warrants further investigation. At high cytokinin concentrations, all genotypes converged toward similarly reduced root growth.

Confocal analysis of TCSn::GFP reporter activity in root cap cells revealed genotype-dependent variation in cytokinin signaling output. The doa10a mutant displayed significantly higher fluorescence intensity compared to *hrd1a hrd1b* and the quadruple mutant, while Col-0 and the quadruple line showed intermediate levels. These findings indicate that specific ERAD components can influence cytokinin signaling intensity in a tissue-dependent manner.

Overall, the results suggest that ERAD pathways contribute to fine-tuning cytokinin signaling and root developmental responses under low hormone conditions, while cytokinin remains the primary regulator of root growth.

Keywords: *Arabidopsis thaliana*, Cytokinin, ER-associated degradation (ERAD), Root development

Table of Contents

1. Introduction **9**
1.1 Cytokinin 9
1.1.1 Biosynthesis and Metabolism 9
1.1.1.1 IPT enzymes 9
1.1.1.2 LOG enzymes 9
1.1.1.3 Active and inactive cytokinin forms 10
1.1.2 CKX-mediated degradation 11
1.1.3 Transport 11
1.1.4 Signaling 12
1.2 Root Development in *Arabidopsis thaliana* 13
1.2.1 Root System Architecture 13
1.2.2 Hormonal Regulation of Root Development 14
1.2.3 Cytokinin-Mediated Regulation of Root Growth 14
1.3 Cytokinin Oxidase/Dehydrogenase (CKX) Enzymes 15
1.3.1 CKX Family in *Arabidopsis* 15
1.3.2 Regulation of Cytokinin Homeostasis 15
1.3.3 Biological Functions of CKX Proteins 16
1.3.4 CKX Mutants and Root Phenotypes 16
1.4 Endoplasmic Reticulum Quality Control (ERQC) and ER-Associated Degradation (ERAD) 16
1.4.1 Protein Folding and Quality Control in the ER 16
1.4.2 Protein Glycosylation 17
1.4.3 ER-Associated Degradation (ERAD) 17
1.4.4 ERAD Components in *Arabidopsis* 17
1.4.5 Functions and Substrates of ERAD 18
1.5 Connection Between ER Quality Control, ERAD, and Cytokinin Regulation 19
1.5.1 ER Quality Control and Hormone-Related Proteins 19
1.5.2 ERAD-Dependent Regulation of Cytokinin Homeostasis: The CKX–HIPP Module 20
1.5.3 Consequences for Root Development 22
2. Objectives and Research Questions **24**
3. Material and Methods **24**
3.1 Genotyping of ERAD Knockout and TCSn::GFP Reporter Lines 24
3.1.1 Plant Material 24
3.1.2 Genomic DNA Extraction 24

3.1.3 PCR-Based Genotyping 24
3.1.4 CAPS Marker Analysis 25
3.1.5 Agarose Gel Electrophoresis 26
3.2 Root Growth Assay under Cytokinin Treatment 27
3.2.1 Media Preparation 27
3.2.2 Seed Sterilization and Planting 28
3.2.3 Growth Conditions and Root Measurement 28
3.3 Confocal Laser Scanning Microscopy (CLSM) 28
3.3.1 Dissection and Staining 28
3.3.2 Imaging 29
3.3.3 Image Processing and Quantification 29
3.4 Construction of a CRISPR/Cas9 Vector for *DOA10A* Targeting 30
3.4.1 *Arabidopsis* thaliana Lines, Genetic Backgrounds and Growth Conditions 30
3.4.2 Cloning of the *DOA10A* CRISPR Construct 31
3.4.3 Transformation into Agrobacterium tumefaciens 33
3.4.4 Floral-Dip Transformation and Selection 34
3.4.5 Selection of Cas9-Free Segregants 34
3.4.6 Genomic DNA Isolation and PCR Verification of Cas9 T-DNA 35
3.5 Statistical Analysis 36
4. Results **37**
4.1 Genotyping of ERAD Mutants and TCSn::GFP Reporter Lines 37
4.1.1 PCR-based Genotyping 37
4.1.2 Restriction Digest (CAPS Marker Analysis) 40
4.2 Root Assays 41
4.2.1 Primary Root Length 41
4.2.2 Lateral Root Number 42
4.3 Confocal Analysis of TCSn::GFP Cytokinin Signaling in ERAD Mutants 45
4.4 Verification of the *DOA10A* CRISPR/Cas9 Construct 47
4.5 Transformation and Selection of Transgenic Lines 49
4.5.1 Identification of Cas9-Free Segregants 51
5. Discussion **52**
5.1 Genotyping of ERAD Mutants and TCSn::GFP Reporter Lines 52
5.2 Root Assays 53
5.3 Confocal Analysis of Cytokinin Signaling 55

5.4 Verification of the *DOA10A* CRISPR/Cas9 Construct and Selection of Transgenic Lines 57
6. Conclusion **59**
References **61**

List of Figures

Figure 1. Subcellular compartmentalization of cytokinin metabolism. 10
Figure 2. Organization of the *Arabidopsis* root. 13
Figure 3. Model of the *Arabidopsis* Hrd1 ERAD complex. 18
Figure 4. Cytokinin signaling and metabolism are spatially compartmentalized within the plant cell. 20
Figure 5. Representative confocal imaging channels used for quantification of TCSn::GFP fluorescence in *doa10a* root cap cells. 30
Figure 6. Schematic map of the CRISPR-Cas9 vector used for *DOA10A* targeting. 31
Figure 7. Plasmid map of the final pAGM55261-*DOA10A* construct. 33
Figure 8. *HRD1B* locus PCR genotyping with gene-specific primers. 38
Figure 9. *HRD1B* locus PCR genotyping with T-DNA-specific primers. 38
Figure 10. *HRD1A* locus PCR genotyping with gene-specific primers. 39
Figure 11. *HRD1A* locus PCR genotyping with T-DNA-specific primers. 39
Figure 12. TCSn::GFP reporter construct amplification by PCR. 40
Figure 13. CAPS marker analysis of *DOA10A* and *DOA10B* alleles in *Arabidopsis thaliana*. 41
Figure 14. Representative root growth phenotype of Col-0 and the quadruple mutant. 43
Figure 15. Primary root length in Col-0 and ERAD mutants under cytokinin treatment. 44
Figure 16. Lateral root number in Col-0 and ERAD mutants under cytokinin treatment. 45
Figure 17. GFP fluorescence intensity in TCSn::GFP reporter lines across ERAD mutant backgrounds. 46
Figure 18. Representative confocal images of TCSn::GFP fluorescence in root cap cells. 47
Figure 19. Colony PCR analysis of the pAGM55261-DOA10A CRISPR/Cas9 construct in transformed E. coli colonies. 48
Figure 20. pAGM55261-DOA10A CRISPR/Cas9 plasmid restriction enzyme analysis based on NotI and NcoI digestion. 48

Figure 21. Representative T4 sub-lines showing segregation of hygromycin-resistant and hygromycin-sensitive seedlings..... 50

Figure 22. PCR-based screening of T_4 *Arabidopsis* thaliana seedlings using Cas9-specific primers 213 and 214..... 51

List of Tables

Table 1. Primer/Assay Overview and PCR Conditions..... 25

Table 2. Restriction Digest (CAPS Marker) Assays for DOA10A and DOA10B 26

Table 3. Primer sequences used for PCR-based genotyping..... 26

Table 4. Oligonucleotides used for cloning of the DOA10A sgRNA target sequence..... 32

Table 5. Segregation analysis of hygromycin-resistant and hygromycin-sensitive seedlings in T-DNA insertion lines derived from line 5-3 sub-lines..... 50

1. Introduction

1.1 Cytokinin

Cytokinins are a class of adenine-derived phytohormones that regulate a wide range of plant developmental processes, including cell division, meristem activity, vascular differentiation, and root system architecture (Mok & Mok, 2001; Kieber & Schaller, 2014). Their concentration and distribution are tightly controlled through biosynthesis, metabolic activation, transport, reversible conjugation, and irreversible degradation (Sakakibara, 2006).

1.1.1 Biosynthesis and Metabolism

Cytokinin homeostasis is regulated through a network of biosynthetic and metabolic pathways that determine the spatial and temporal availability of active hormone forms. **T**his metabolic network and its subcellular distribution are shown in Figure 1.

1.1.1.1 IPT enzymes

The initial and rate-limiting step of cytokinin biosynthesis is catalyzed by isopentenyl transferase (IPT) enzymes. IPTs transfer an isopentenyl group from dimethylallyl diphosphate (DMAPP) to adenosine phosphates (ATP, ADP, or AMP), producing cytokinin nucleotides as primary biosynthetic products. In *Arabidopsis thaliana*, IPT gene family members show tissue-specific expression patterns and distinct developmental functions (Miyawaki et al., 2006).

1.1.1.2 LOG enzymes

Cytokinin nucleotides produced by IPT activity are generally inactive precursors. Their conversion into biologically active free-base cytokinins is catalyzed by LONELY GUY (LOG) enzymes, which directly activate cytokinin nucleotides by removing the ribose-5'-monophosphate group. This reaction provides a local and rapid mechanism for cytokinin activation in specific tissues (Kurakawa et al., 2007; Kuroha et al., 2009).

1.1.1.3 Active and inactive cytokinin forms

Cytokinins exist in multiple interconvertible molecular forms with distinct biological activities. The major active forms include trans-zeatin (tZ), isopentenyladenine (iP), cis-zeatin (cZ), and dihydrozeatin (DHZ), which are perceived by cytokinin receptors and activate downstream signaling pathways. In contrast, cytokinin nucleotides serve as biosynthetic intermediates, ribosides function in transport, and glucosylated forms act as storage or irreversible inactivation products, collectively contributing to cytokinin homeostasis (Sakakibara, 2006; Kieber & Schaller, 2014).

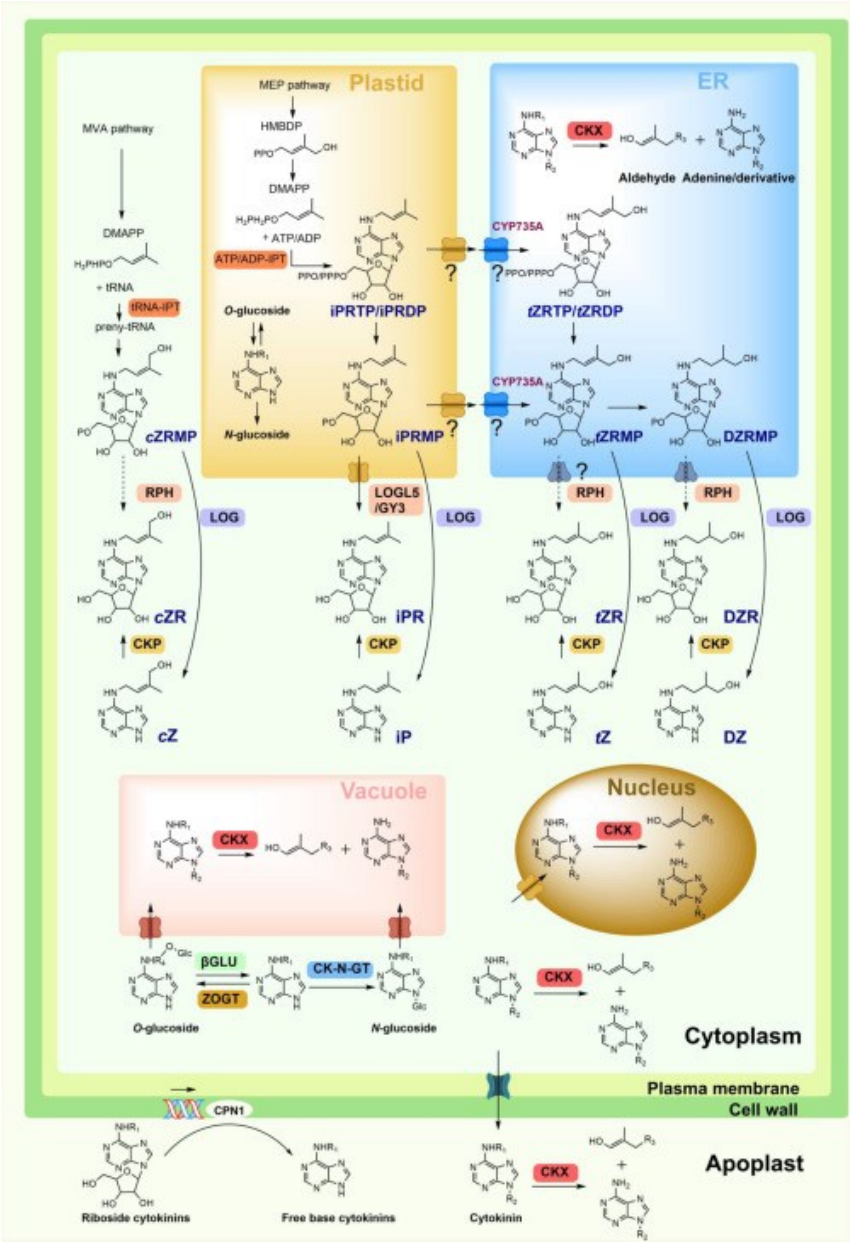

Figure 1. Subcellular compartmentalization of cytokinin metabolism. Cytokinin interconversion (cZ, iP, tZ, DZ and their nucleotide, riboside, and glucoside forms) occurs across the plastid, ER, vacuole, nucleus, and apoplast, with CKX-mediated degradation acting in multiple compartments. Reproduced from Zhao et al. (2024), *Plant Communications*, https://doi.org/10.1016/j.xplc.2024.100936. Licensed under CC BY-NC-ND 4.0.

1.1.2 CKX-mediated degradation

Irreversible degradation of cytokinins is mediated by cytokinin oxidase/dehydrogenase (CKX) enzymes, which catalyze the oxidative cleavage of the N6-side chain of isoprenoid cytokinins. This reaction represents a key regulatory mechanism controlling cytokinin levels in plants. The CKX gene family in *Arabidopsis thaliana* consists of multiple members with distinct expression patterns and subcellular localization (Schmülling et al., 2003; Werner et al., 2003). Altered CKX activity has been shown to strongly affect plant development, particularly root meristem size, lateral root formation, and overall root architecture (Werner et al., 2010; Kieber & Schaller, 2014).

1.1.3 Transport

Cytokinins are synthesized in spatially restricted tissues but function throughout the plant, requiring both local and long-distance transport to coordinate developmental processes. In particular, roots represent a major site of cytokinin biosynthesis, from where hormones are transported to aerial tissues to regulate shoot growth and development, while shoot-derived signals can also influence root physiology (Sakakibara, 2006; Hirose et al., 2008; Kieber & Schaller, 2018).

Long-distance cytokinin transport occurs mainly through the xylem and phloem and is dependent on the chemical form of the hormone. Trans-zeatin (tZ)-type cytokinins are predominantly transported from roots to shoots via the xylem and represent a major root-to-shoot signal. In contrast, isopentenyladenine (iP)-type cytokinins are more abundant in the phloem and are thought to contribute to shoot-to-root communication (Sakakibara, 2006; Hirose et al., 2008).

Cytokinin movement across membranes is mediated by specific transport proteins. The ATP-binding cassette transporter ABCG14 is essential for loading tZ-type cytokinins into the xylem for root-to-shoot translocation, and its loss leads to severely reduced shoot growth due to impaired cytokinin transport (Ko et al., 2014). In addition, PURINE PERMEASE (PUP) and EQUILIBRATIVE NUCLEOSIDE TRANSPORTER (ENT) family members contribute to cellular uptake and distribution of cytokinin-related compounds, thereby modulating local hormone availability (Burkle et al., 2003; Zürcher et al., 2016).

Together, these transport mechanisms establish cytokinin gradients between tissues, which are further refined by local biosynthesis and degradation. These gradients are essential for coordinating developmental processes such as meristem activity and root system architecture (Bishopp et al., 2011; Kieber & Schaller, 2018).

1.1.4 Signaling

Cytokinin signaling is mediated by a multistep two-component phosphorelay system that is evolutionarily related to bacterial histidine kinase signaling pathways. This system enables plants to perceive cytokinin levels and translate them into transcriptional responses that regulate growth and development (Hwang et al., 2012; Kieber & Schaller, 2018).

Cytokinin perception is mediated by membrane-associated ARABIDOPSIS HISTIDINE KINASE (AHK) receptors, which in *Arabidopsis* are predominantly localized at the endoplasmic reticulum and, to a lesser extent, at the plasma membrane, linking cytokinin availability in specific subcellular compartments to signaling output (Wulfetange et al., 2011; Caesar et al., 2011).

The signal is subsequently transferred via ARABIDOPSIS HISTIDINE PHOSPHOTRANSFER PROTEINS (AHPs) to the nucleus, where it regulates the activity of ARABIDOPSIS RESPONSE REGULATORS (ARRs). Type-B ARRs function as transcriptional activators of cytokinin-responsive genes, while type-A ARRs act as negative feedback regulators, ensuring controlled signal output (Hutchison et al., 2006; To et al., 2004; Argyros et al., 2008).

Through this phosphorelay system, cytokinin regulates key developmental processes including meristem activity, cell differentiation, and root system architecture (Hwang et al., 2012; Kieber & Schaller, 2018). The core components of this pathway are illustrated in Figure 4.

1.2 Root Development in *Arabidopsis thaliana*

The root system of *Arabidopsis thaliana* provides a well-established model for studying plant development due to its simple architecture and continuous growth. The root system consists of a primary root and a variable number of lateral roots, which together determine the overall root system architecture and influence nutrient uptake, water acquisition, and plant stability (Benfey and Scheres, 2000; Péret et al., 2009).

1.2.1 Root System Architecture

The primary root is formed during embryogenesis and grows through the activity of the root apical meristem (RAM), which contains a population of stem cells surrounding the quiescent center. These stem cells continuously divide to generate new cells that undergo elongation and differentiation, enabling root growth along the longitudinal axis (Dolan et al., 1993; Scheres et al., 2002). The organization of the root tip and its developmental zones is shown in Figure 2.

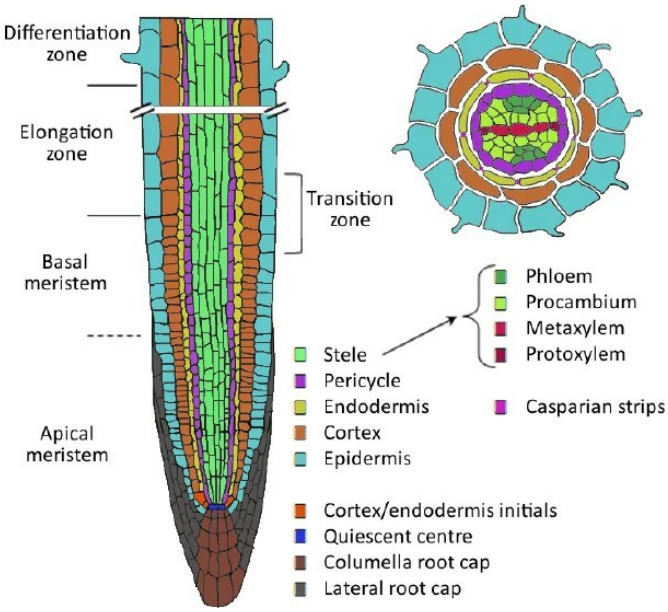

Figure 2. Organization of the *Arabidopsis* root. (Left) Longitudinal section showing the concentric tissue layers and developmental zones along the root axis. (Right) Cross-section at the differentiated root zone, showing root hairs and Casparian strips. Reproduced from De Smet et al. (2015), *International Journal of Molecular Sciences* 16:19195–19224, https://doi.org/10.3390/ijms160819195. Licensed under CC BY 4.0.

Lateral roots originate post-embryonically from pericycle cells and are initiated in a highly regulated pattern influenced by both intrinsic developmental programs and environmental signals. Their formation contributes significantly to the plasticity of the root system architecture and allows plants to adapt to changing environmental conditions (Malamy and Benfey, 1997; Péret et al., 2009).

1.2.2 Hormonal Regulation of Root Development

Root development is tightly controlled by phytohormones, with auxin and cytokinin playing central but antagonistic roles. Auxin promotes root meristem activity and lateral root initiation, whereas cytokinin generally acts as a negative regulator of primary root growth by restricting meristem size and promoting differentiation (Aloni et al., 2006; Müller and Sheen, 2008).

The balance between auxin and cytokinin signaling is therefore a key determinant of root system architecture. Cytokinin modulates auxin distribution and signaling components, thereby influencing cell division rates in the root meristem and the initiation of lateral root primordia (Bishopp et al., 2011; Ruzicka et al., 2009).

1.2.3 Cytokinin-Mediated Regulation of Root Growth

Cytokinin regulates root development primarily by controlling cell proliferation and differentiation within the root apical meristem. Elevated cytokinin levels reduce meristem size by promoting the transition from cell division to differentiation, whereas reduced cytokinin activity leads to an enlarged meristem and enhanced primary root growth (Werner et al., 2003; Dello Ioio et al., 2007).

In addition, cytokinin negatively regulates lateral root formation by inhibiting the early stages of lateral root primordium initiation and development. This regulation

ensures proper spacing and density of lateral roots, contributing to optimized root system architecture under varying environmental conditions (Laplaze et al., 2007; Chang et al., 2015).

Through these mechanisms, cytokinin acts as a key regulator of root growth dynamics, integrating developmental and environmental signals to fine-tune root system architecture.

1.3 Cytokinin Oxidase/Dehydrogenase (CKX) Enzymes

Cytokinin oxidase/dehydrogenase (CKX) enzymes are responsible for the irreversible degradation of cytokinins and therefore represent a key regulatory mechanism controlling cytokinin homeostasis in plants. By catalyzing the cleavage of the N6-side chain of isoprenoid cytokinins, CKXs reduce the levels of biologically active cytokinin forms and thereby modulate growth and developmental processes (Schmülling et al., 2003; Werner et al., 2003).

1.3.1 CKX Family in *Arabidopsis*

In *Arabidopsis thaliana*, the CKX gene family consists of multiple members (CKX1–CKX7), which differ in expression patterns, substrate specificity, and subcellular localization. CKX proteins are localized to distinct subcellular compartments, including the endoplasmic reticulum, vacuole, and apoplast, depending on the isoform (Schmülling et al., 2003; Werner et al., 2006). Notably, CKX1 is a type II single-pass ER membrane protein, establishing it as a genuine ER-resident client of the secretory quality-control machinery rather than a protein that merely transits the ER en route elsewhere (Niemann et al., 2018). This ER and apoplastic localization of CKX proteins is depicted in Figure 4.

1.3.2 Regulation of Cytokinin Homeostasis

CKX enzymes act as major determinants of cytokinin concentration by balancing biosynthesis and degradation. Their activity ensures spatial and temporal control of cytokinin levels, thereby contributing to the formation of cytokinin gradients across tissues. Alterations in CKX expression or activity lead to significant changes in

cytokinin accumulation and signaling output (Werner et al., 2003; Kieber & Schaller, 2014).

1.3.3 Biological Functions of CKX Proteins

CKX-mediated cytokinin degradation plays a central role in regulating plant development, particularly in meristem activity, organ formation, and root system architecture. Reduced CKX activity generally leads to elevated cytokinin levels, resulting in smaller root meristems and reduced primary root growth, whereas increased CKX activity enhances root growth by lowering cytokinin concentrations (Werner et al., 2010; Kieber & Schaller, 2014).

1.3.4 CKX Mutants and Root Phenotypes

Genetic studies in *Arabidopsis* have demonstrated that CKX loss-of-function mutants display elevated cytokinin levels and corresponding developmental phenotypes, including reduced root elongation and altered lateral root formation. Conversely, overexpression of CKX genes results in cytokinin deficiency phenotypes characterized by enhanced root growth and reduced shoot development, highlighting the importance of CKX enzymes in maintaining hormonal balance (Werner et al., 2003; Werner et al., 2010).

1.4 Endoplasmic Reticulum Quality Control (ERQC) and ER-Associated Degradation (ERAD)

Proteins destined for secretion or membrane localization are synthesized and folded in the endoplasmic reticulum (ER), where protein homeostasis (proteostasis) is tightly controlled. The ER quality control (ERQC) system ensures that only properly folded proteins are exported to their final destinations, while misfolded or unassembled proteins are retained and targeted for degradation (Strasser, 2018; Liu and Howell, 2016).

1.4.1 Protein Folding and Quality Control in the ER

Within the ER lumen, nascent proteins undergo folding assisted by molecular chaperones, folding enzymes, and lectin-based quality control systems. Misfolded

proteins are recognized by ERQC mechanisms and retained in the ER to prevent trafficking of dysfunctional proteins through the secretory pathway. This system is essential for maintaining cellular homeostasis and protein functionality (Strasser, 2018).

1.4.2 Protein Glycosylation

N-linked glycosylation is a central component of ER protein quality control in plants. Glycan structures attached to nascent proteins serve as folding tags that are monitored by ER-resident lectin chaperones. Processing of these glycans determines whether a protein will be correctly folded and exported or retained for degradation. This glycan-dependent surveillance system is tightly integrated into ERQC mechanisms (Strasser, 2018).

1.4.3 ER-Associated Degradation (ERAD)

ER-associated degradation (ERAD) eliminates misfolded or unassembled proteins that fail ER quality control. In this pathway, target proteins are recognized in the ER, retrotranslocated into the cytosol, ubiquitinated, and degraded by the 26S proteasome. ERAD is therefore essential for maintaining ER homeostasis and preventing toxic protein accumulation (Christianson and Ye, 2014; Liu and Howell, 2016).

1.4.4 ERAD Components in *Arabidopsis*

In *Arabidopsis thaliana*, ERAD is mediated by conserved ubiquitin–proteasome system components. Substrate recognition and ubiquitination are carried out by the ER membrane-embedded E3 ubiquitin ligases *HRD1A/HRD1B* and DOA10A/DOA10B, which define two partially redundant ERAD branches with overlapping and distinct substrate preferences (Liu and Howell, 2016; Strasser, 2018). Ubiquitination requires the E2 conjugating enzyme UBC32, and extraction of ubiquitinated substrates from the ER membrane into the cytosol for proteasomal delivery is carried out by the AAA-ATPase CDC48, acting together with its cofactors (Liu and Howell, 2016; Strasser, 2018). Additional plant-specific ERAD components have also been identified, including EBS7, a conserved ER membrane-

localized factor required for degradation of specific ERAD substrates (Liu and Howell, 2016).

These ERAD components are essential for plant development and stress responses. Loss of ERAD function leads to accumulation of misfolded proteins in the ER, activation of stress responses, and developmental defects, highlighting the importance of ER protein quality control for normal plant growth (Liu and Howell, 2016; Strasser, 2018). The core architecture of this complex is illustrated in Figure 3.

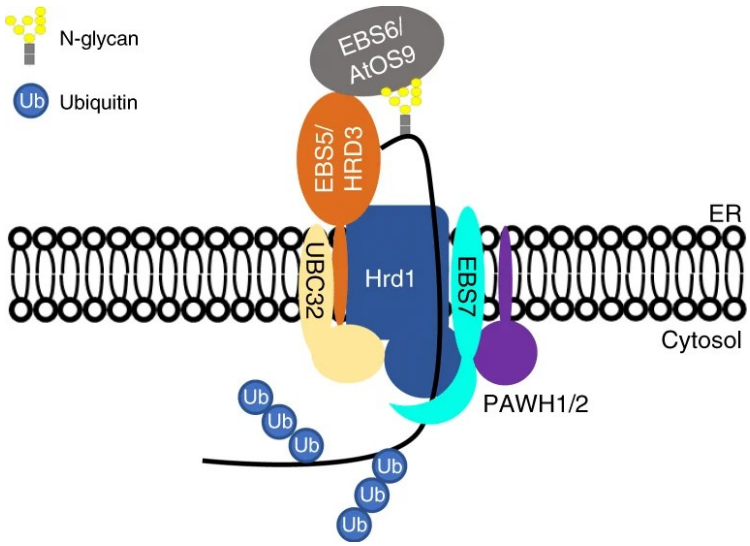

Figure 3. Model of the *Arabidopsis HRD1* ERAD complex. An ERAD-L substrate is recognized via N-glycan trimming (EBS6/AtOS9) and recruited to the membrane-embedded ligase *HRD1*, together with EBS5/HRD3, UBC32, EBS7, and PAWH1/2, leading to substrate polyubiquitination. Reproduced from Lin et al. (2019), *Nature Communications* 10:3492, https://doi.org/10.1038/s41467-019-11480-7. Licensed under CC BY 4.0.

1.4.5 Functions and Substrates of ERAD

ERAD targets a wide range of substrates, including misfolded secretory proteins, membrane proteins, and glycoproteins. In plants, ERAD is also linked to the regulation of key signaling pathways, as several hormone-related proteins and receptors depend on ER quality control for proper folding, stability, or turnover. This suggests a functional connection between ERAD and hormone homeostasis pathways (Strasser, 2018; Liu and Howell, 2016).

1.5 Connection Between ER Quality Control, ERAD, and Cytokinin Regulation

Cytokinin homeostasis is regulated at multiple levels, including biosynthesis, transport, degradation, and intracellular protein quality control. Because several enzymes and receptors involved in hormone metabolism are membrane-associated or enter the secretory pathway, their proper folding and stability depend on the endoplasmic reticulum (ER) protein quality control system (ERQC) (Strasser, 2018; Liu and Howell, 2016).

1.5.1 ER Quality Control and Hormone-Related Proteins

The ERQC system ensures correct folding of secretory and membrane proteins through chaperone-assisted folding and glycoprotein quality control. Proteins that fail to achieve proper folding are retained in the ER and targeted for degradation via the ER-associated degradation (ERAD) pathway. This system is essential for maintaining proteostasis and cellular function in plants (Strasser, 2018; Christianson and Ye, 2014).

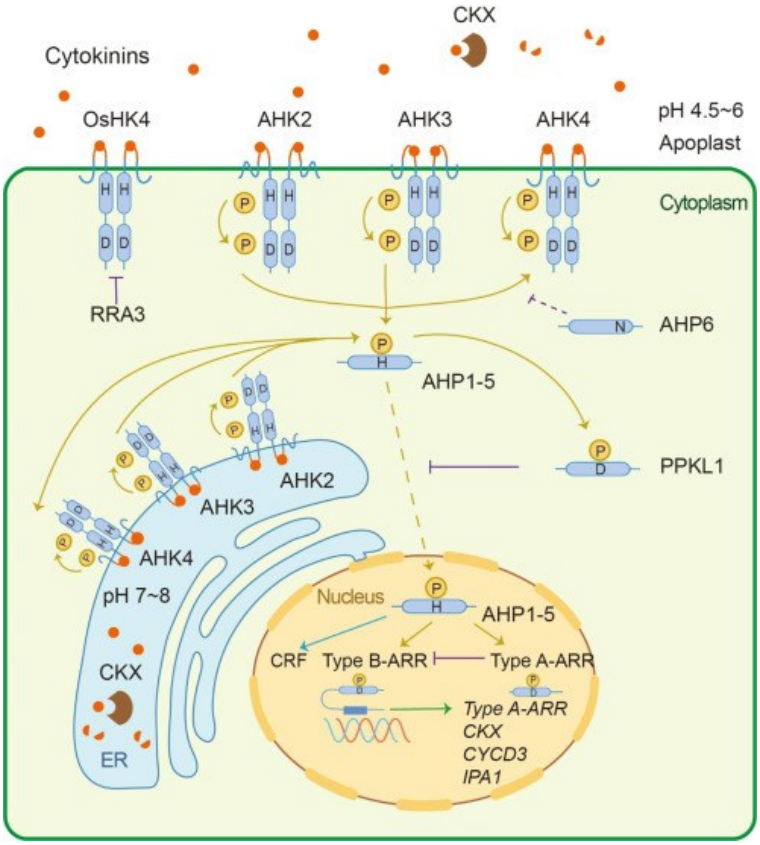

Figure 4. Cytokinin signaling and metabolism are spatially compartmentalized within the plant cell. Cytokinin receptors (e.g., AHK2–AHK4, OsHK4) are localized predominantly at the ER membrane, initiating a two-component phosphorelay (AHP1–5) that activates type-A and type-B ARR transcription factors in the nucleus. Cytokinin oxidase/dehydrogenase (CKX) proteins are also present at the ER and apoplast, where pH-dependent activity contributes to cytokinin degradation. Reproduced from Zhao et al. (2024), *Plant Communications*, https://doi.org/10.1016/j.xplc.2024.100936. Licensed under CC BY-NC-ND 4.0.

As illustrated in Figure 4, both cytokinin perception (via ER-localized AHK receptors) and cytokinin degradation (via CKX) occur at the endoplasmic reticulum, placing CKX directly within reach of the ER's protein quality-control machinery — the structural basis for ERAD-mediated regulation of CKX turnover and, in turn, cytokinin homeostasis, discussed further in Section 1.5.2.

1.5.2 ERAD-Dependent Regulation of Cytokinin Homeostasis: The CKX–HIPP Module

A direct mechanistic link between ERAD and cytokinin homeostasis was established by Niemann et al. (2018), who showed that cellular CKX protein levels are controlled by ERQC/ERAD, with significant consequences for cytokinin signaling output. Building on this, Guo et al. (2021) identified the molecular components that regulate this process. Using a yeast two-hybrid screen with CKX1 as bait, they found that heavy metal-associated isoprenylated plant proteins (HIPPs) interact specifically with CKX proteins synthesized in the ER. CKX–HIPP protein complexes were detected both at the ER membrane and in the cytosol, consistent with a role for HIPPs in the retrotranslocation step of CKX ERAD (Guo et al., 2021).

Functional evidence supported this model: HIPP overexpression and higher-order hipp loss-of-function mutants both altered steady-state CKX protein levels, indicating that the studied HIPPs act as regulators of CKX turnover via ERAD. These changes in CKX abundance produced corresponding shifts in cytokinin signaling activity and typical cytokinin-related morphological phenotypes, directly linking ERAD-mediated CKX turnover to hormone output at the whole-plant level. Interestingly, HIPP gene expression was itself transcriptionally repressed by cytokinin, suggesting a feedback loop in which cytokinin signaling modulates its own degradation capacity by tuning ERAD activity toward CKX. Loss of HIPP function additionally activated the unfolded protein response and compromised ER stress tolerance, indicating that HIPPs function as genuine components of the plant ERAD machinery rather than as CKX-specific accessory factors alone (Guo et al., 2021).

Together, these findings establish that ERAD-mediated turnover of CKX is a bona fide regulatory node in cytokinin homeostasis. However, Guo et al. (2021) approached this system primarily from the substrate-adaptor side (CKX and HIPPs), and the contribution of the core ERAD machinery itself — the E3 ligases *HRD1A/HRD1B* and *DOA10A/DOA10B*, the E2 enzyme UBC32, and the retrotranslocation motor CDC48 — to CKX turnover and cytokinin-dependent root phenotypes has not been directly tested. Whether disruption of these core components phenocopies the effects of HIPP dysregulation, and how this manifests

specifically in root system architecture, remains an open question that this thesis addresses.

1.5.3 Consequences for Root Development

Because cytokinin is a key regulator of root meristem activity and lateral root formation, any process affecting cytokinin homeostasis can influence root system architecture. Changes in CKX activity alter cytokinin levels, thereby affecting the balance between cell division and differentiation in the root apical meristem. Consequently, ERAD-dependent effects on CKX turnover are expected to propagate into measurable changes in root growth dynamics through modulation of cytokinin signaling output (Werner et al., 2003; Dello Ioio et al., 2007; Kieber & Schaller, 2018).

2. Objectives and Research Questions

The aim of this study is to investigate the role of core ER-associated degradation (ERAD) components in cytokinin-regulated root development in *Arabidopsis thaliana*. Building on evidence that the HIPP–CKX module links ERAD to cytokinin homeostasis (Guo et al., 2021), this work focuses on testing whether disruption of the core ERAD machinery similarly affects CKX-dependent cytokinin regulation and, consequently, root growth dynamics.

We hypothesize that disruption of core ERAD components (*HRD1A/B, DOA10A/B*) alters the abundance, localization, and/or activity of ER-associated CKX proteins, thereby perturbing cytokinin homeostasis and signaling output in roots. Depending on whether ERAD loss stabilizes catalytically active CKX or leads to accumulation of inactive or mislocalized CKX species, ERAD-deficient lines are expected to display either cytokinin-deficiency-like or cytokinin-overaccumulation-like root phenotypes.

To address this aim, the following research questions are formulated:

1. Does loss of function of core ERAD components (*HRD1A/B, DOA10A/B*) alter primary root growth and lateral root formation in *Arabidopsis thaliana*

compared to wild type, under both standard and cytokinin-supplemented conditions?

2. Do the root phenotypes observed in ERAD-deficient lines correspond to altered cytokinin signaling output, as assessed using the TCSn::GFP reporter?
3. Are the observed root and signaling phenotypes consistent with a cytokinin-deficiency-like or a cytokinin-overaccumulation-like state, and how does this inform the relationship between ERAD activity and CKX-dependent cytokinin regulation in roots?

3. Material and Methods

3.1 Genotyping of ERAD Knockout and TCSn::GFP Reporter Lines

3.1.1 Plant Material

Leaf samples were collected from *Arabidopsis thaliana* grown in standard growth conditions; Tissue from the selected genotypes was sampled for genomic DNA extraction and PCR-based genotyping.

3.1.2 Genomic DNA Extraction

Genomic DNA was extracted from *Arabidopsis thaliana* leaves with a rapid extraction protocol adapted from (Neff et al. 1998); One or two leaves were harvested and finely ground in a 1.5 mL microcentrifuge tube with 500 µL extraction buffer (200 mM Tris-HCl, pH 7.5; 250 mM NaCl; 25 mM EDTA, pH 8.0; 0.5% SDS). Samples were centrifuged at 13,000 rpm for 2 min and supernatant was transferred to a new tube.

The supernatant was mixed with 450 µL isopropanol and centrifuged at 13,000 rpm for 20 min to precipitate DNA. The DNA pellet was washed with 1 mL of 70% ethanol and re-centrifuged for 2 min.

The pellet was air-dried after removal of the ethanol and resuspended in 50 µL TE buffer (10 mM Tris-HCl, pH 7.5; 1 mM EDTA, pH 8.0). The DNA samples were stored at −20 °C until use.

3.1.3 PCR-Based Genotyping

Genotyping was done by PCR using gene-specific and T-DNA specific primer combinations to identify the presence of *hrd1a, hrd1b, doa10a, doa10b*, and TCSn::GFP alleles.

PCR reactions were carried out in a final volume of 20 µL using BioZtaq DNA polymerase, the enzyme's supplied reaction buffer, dNTPs, gene-specific primers and 2 µL of genomic DNA template. Annealing temperature was optimized for each primer pair and varied between 53 and 58.5 °C.

Agarose gel electrophoresis was used to analyze the PCR products. The obtained band patterns were used to determine the genotype of the respective *hrd1a, hrd1b, doa10a, doa10b* and TCSn::GFP lines.

Assay	**Locus**	**Primers (ID)**	**Anneal (°C; time)**	**Extension**	**PCR Type**
PCR1	*HRD1B*	F=70, R=71	54°C; 00:45	72°C; 01:00	Gene-specific
PCR2	*HRD1B*	F=13, R=71	55°C; 00:45	72°C; 01:00	T-DNA-specific
PCR3	TCSn::GFP	F=215, R=216	58.5°C; 00:45	72°C; 01:00	Reporter Detection
PCR4	*HRD1A*	F=68, R=69	56°C; 00:40	72°C; 01:00	gene-specific
PCR5	*HRD1A*	F=69, R=13	55°C; 00:45	72°C; 01:00	T-DNA-specific
PCR6	*DOA10B*	F=590, R=591	53°C; 00:50	72°C; 01:00	CAPS Marker
PCR7	*DOA10A*	F=587, R=588 (~790 bp)	53°C; 00:50	72°C; 01:00	CAPS Marker

Table 1. Primer/Assay Overview and PCR Conditions.

3.1.4 CAPS Marker Analysis

Wild type and mutant alleles of *DOA10A* and *DOA10B* were distinguished by Cleaved Amplified Polymorphic Sequence (CAPS) marker analysis. The genomic regions carrying the polymorphic sites were amplified using gene-specific primers and were digested with the appropriate restriction enzymes (New England Biolabs). The resulting fragments were then separated on 1.5% agarose gels and visualized in comparison to wild-type and H2O controls. Genotypes were assigned based on restriction fragment patterns, taking into account the presence or absence of the respective restriction sites.

Assay	Target Locus	Primers (ID / Fragment Size)	Restriction Enzyme	Buffer (Type / Conc.)	Incubation Conditions
CAPS-1	*DOA10B* – allelic verification	F = 590, R = 591 (~750 bp)	BsrDI	r2.1 buffer (10×, NEB)	37 °C for 1 h → 1.5 % agarose gel
CAPS-2	*DOA10A* – allelic verification	F = 587, R = 588 (~790 bp)	EagI	CutSmart buffer (10×, NEB)	37 °C for 1 h → 1.5 % agarose gel

Table 2. Restriction Digest (CAPS Marker) Assays for *DOA10A* and *DOA10B*.

3.1.5 Agarose Gel Electrophoresis

PCR products were analyzed by electrophoresis on an agarose gel. Agarose gels either 0.8% or 1.5% (w/v) in 1× TAE buffer were prepared depending on the size of the fragments. Samples were mixed with loading dye before loading and run on electrophoresis.

The DNA fragments were visualized using Midori Green Advance under UV illumination and the fragment sizes were estimated using an appropriate DNA ladder.

Primer Name	Sequence (5′→3′)
HRD1A-F (68)	AACGACAGGTTTCCTGATGC
HRD1A-R (69)	CCCTGGTTACCTGAGCTTGA
HRD1A-F (T-DNA, 69)	AACGACAGGTTTCCTGATGC
HRD1A-R (T-DNA, 13)	CCCTGGTTACCTGAGCTTGA
HRD1B-F (70)	TCAATGGGAAGGAAAACCAG
HRD1B-R (71)	AGTTCTTCAGGAGTTGCATCAG

HRD1B-F (T-DNA, 13)	ATTTTGCCGATTTCGGAAC
HRD1B-R (T-DNA, 71)	AGTTCTTCAGGAGTTGCATCAG
DOA10A-F (587)	atttaaggcccaaacccaac
DOA10A-R (588)	tgcaattgcccattcattta
DOA10B-F (590)	agttcccggaaATGGAGATT
DOA10B-R (591)	AGAACTCGGGGTGTCTCCTT
GFP-F (215)	TGTTCCATGGCCAACACTTG
GFP-R (216)	CCATGTGTAATCCCAGCAGC

Table 3. Primer sequences used for PCR-based genotyping.

3.2 Root Growth Assay under Cytokinin Treatment

3.2.1 Media Preparation

Seeds of *Arabidopsis thaliana* were cultured on Murashige and Skoog (MS) medium supplemented with three concentrations of benzyladenine (BA) (0 nM (control), 10 nM and 50 nM) for cytokinin sensitivity assays; A total of 36 square Petri plates (4 genotypes x 3 concentrations x 3 replicates) were used for the analysis of four genotypes in three biological replicates each of the treatments.

MS medium was prepared according to Murashige and Skoog (1962) and supplemented with 1% (w/v) sucrose, 0.8% (w/v) agar and adjusted to pH 5.7 before autoclaving.

After cooling to about 55 °C, BA stock solutions were added to the medium, which was poured into square Petri plates (12 × 12 cm) and left to solidify under sterile conditions.

3.2.2 Seed Sterilization and Planting

Seeds were sterilized for in vitro cultivation of *Arabidopsis* in 800 µL of 70% ethanol containing 0.01% Triton X-100 detergent; Surface contamination was eliminated by sterilization in 1.5 mL reaction tubes for 7 minutes with gentle shaking. Seeds were washed 3 times with 70% ethanol after sterilization and placed on sterile filter paper in a laminar-flow hood to air-dry for approximately 10 min.

Dried seeds were picked up individually with sterile toothpicks soaked in agar and placed on square 12 x 12 cm MS plates in a horizontal line ~2 cm from the top edge with a maximum of 15 seeds per row of 5 Col-0 seeds and 10 mutant seeds. The plates were sealed with Leucopor® tape and closed bottom in a U-shape with Parafilm®, to avoid dessication.

3.2.3 Growth Conditions and Root Measurement

The plates containing seeds were placed in darkness at 4 °C for 3 days to synchronize germination. After that, the plates were placed in a growth chamber at 22 °C under 16 h light / 8 h dark for germination and root growth. Plates were turned vertically for downward root growth. The root tips were marked after 4 days of growth in light to monitor elongation.

After 6 days of growth, the plates were photographed using a digital Camera. Primary root length was measured using ImageJ /Fiji software (Schindelin et al. 2012); Primary root length was measured from the position marked on day 4 after transfer to light to the root tip. Only actively growing seedlings with synchronized germination were included in the analysis. Lateral roots were counted manually under the stereomicroscope on the same seedlings.

3.3 Confocal laser scanning microscopy (CLSM)

3.3.1 Dissection and staining

Seedlings were grown and prepared under the same conditions as described in the root growth assay, using three biological replicates for each genotype. *Arabidopsis*

was cultivated in standard imaging conditions (Murashige & Skoog, 1962); Once the roots were at the proper developmental stage (after 3 days in the dark and 6 days in the growth chamber with 16 h light and 8 h darkness), they were stained with Ethidium Bromide (EtBr) for visualization of cell outlines and to improve visibility of the root cap during confocal imaging. Seedlings were stained by short soaking in EtBr solution. Then the seedlings were rinsed in distilled water and mounted. The roots were then placed in distilled water on microscope slides for imaging.

3.3.2 Imaging

Confocal imaging was performed using a Confocal Laser Scanning Microscope (CLSM) Leica TCS SP5 (Leica Microsystems GmbH, Wetzlar, Germany); GFP fluorescence was detected with a 488 nm excitation laser and emission detection window of 500-550 nm based on previously established imaging settings for GFP in *Arabidopsis* roots. Ethidium Bromide counterstaining was used to visualize cell outlines and the structure of the root tissue. Microscopy and image acquisition was carried out using Leica LASX software; All samples were imaged under the same acquisition settings for comparison between genotypes.

3.3.3 Image processing and quantification

Images were processed and quantified using ImageJ software (Fiji) (Schindelin et al., 2012); Background subtraction, region-of-interest (ROI) selection and fluorescence intensity measurement were performed using the same workflow for all samples and for all replicates. For each seedling, fluorescence intensity was measured within the same root cap region of interest to enable comparison between genotypes.

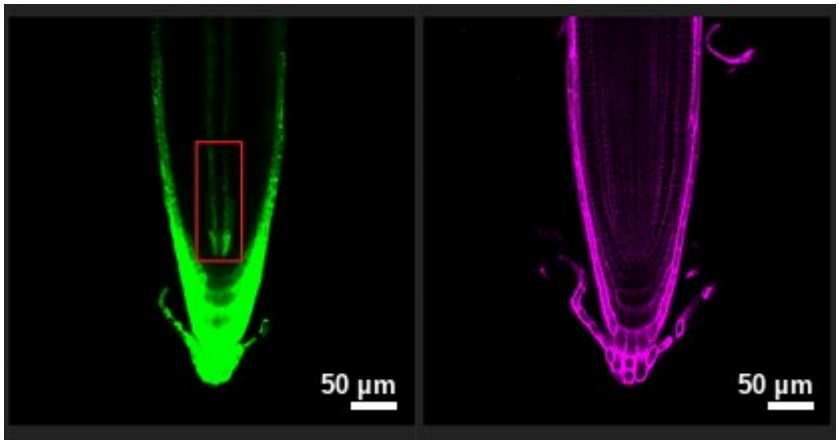

Figure 5. Representative confocal imaging channels used for quantification of TCSn::GFP fluorescence in *doa10a* root cap cells. GFP fluorescence (left) and Ethidium Bromide counterstain showing cell outlines (right). Red rectangle indicates the region of interest (ROI) used for fluorescence intensity quantification in ImageJ/Fiji. Scale bars = 50 µm.

3.4 Construction of a CRISPR/Cas9 Vector for *DOA10A* Targeting

3.4.1 *Arabidopsis thaliana* Lines, Genetic Backgrounds and Growth Conditions

The *Arabidopsis thaliana* ecotype Columbia-0 (Col-0) served as the wild-type reference background for CRISPR/Cas9-mediated genome editing. The recipient genotype for mutant generation was a Cas9-free *doa10b*-3 line in the *ckx3 ckx5* mutant background carrying the pCKX3::CKX3-VENUS transgene.

To obtain *doa10a doa10b* double mutant lines, a CRISPR/Cas9 construct targeting the *DOA10A* gene (At4g34100) was transformed into this genetic background by Agrobacterium-mediated transformation. The line used as the recipients already contained resistance markers for BASTA and kanamycin, therefore these antibiotics were not suitable for the selection of newly transformed plants. The pAGM55261 vector used in this study carries a FAST fluorescent seed-selection marker that can be used to identify transgenic seeds in subsequent generations, independent of antibiotic resistance markers (Shimada et al., 2010; Grützner et al., 2021).

Plants were grown at 22 °C under controlled long-day conditions (16 h light/8 h dark) and used for Agrobacterium-mediated floral-dip transformation.

3.4.2 Cloning of the *DOA10A* CRISPR Construct

A single-guide RNA (sgRNA) was designed using CRISPR-P (Lei et al., 2014) to target an exon of *DOA10A*. Complementary oligonucleotides corresponding to the sgRNA target sequence were annealed together to make a double-stranded DNA insert by incubation at 95 °C for 5 min.

The sgRNA insert was ligated into the pAGM55261 in a 20 µL reaction containing 2 µL vector DNA, 2 µL annealed sgRNA insert, 2 µL ligase buffer (10×), 1 µL ligase, and 13 µL ddH_2O. The The ligation reaction was incubated for 1 h at room temperature and then 20 min at 60 °C.

The pAGM55261 vector consists of an expression cassette for an intron-optimized Cas9 (zCas9i), a BAR selection cassette for glufosinate resistance (BASTA) and a FAST fluorescent seed-selection marker system (Grützner et al., 2021). The ligation products were transformed into competent *Escherichia coli* cells and plated on LB agar with kanamycin (50 µg mL-1).

Figure 6. Schematic map of the CRISPR-Cas9 vector used for *DOA10A* targeting. The vector is based on pAGM55261 (Grützner et al., 2021). Major functional elements relevant for plant transformation and selection are indicated in the map. Reproduced from Grützner et al. (2021), *Plant Communications* 2:100135, https://doi.org/10.1016/j.xplc.2020.100135. Licensed under CC BY-NC-ND 4.0.

Positive colonies were screened by colony PCR using sgRNA flanking primers to verify insertion of the sgRNA sequence into the pAGM55261 vector. PCR products were analyzed by agarose gel electrophoresis and colonies with the expected amplicon size were selected for further analysis.

Plasmid DNA from positive *Escherichia coli* colonies was isolated using a standard alkaline lysis miniprep method. To verify correct plasmid assembly, restriction enzyme digestion using NotI and NcoI was performed, yielding the expected fragment sizes of approximately 13,400 bp and 3,891 bp.

The verified constructs were then introduced into Agrobacterium tumefaciens for plant transformation. Positive Escherichia coli colonies with the verified construct were cultured and stored as 50% glycerol stocks at −80 °C for long term storage.

Oligonucleotide	**Sequence (5′→3′)**
DOA10A-sgRNA-3-1	ATTGGCACGATAACAACACCA
DOA10A-sgRNA-3rv	AAACTGGTGTTGTTATCGTGCCA

Table 4. Oligonucleotides used for cloning of the *DOA10A* sgRNA target sequence.

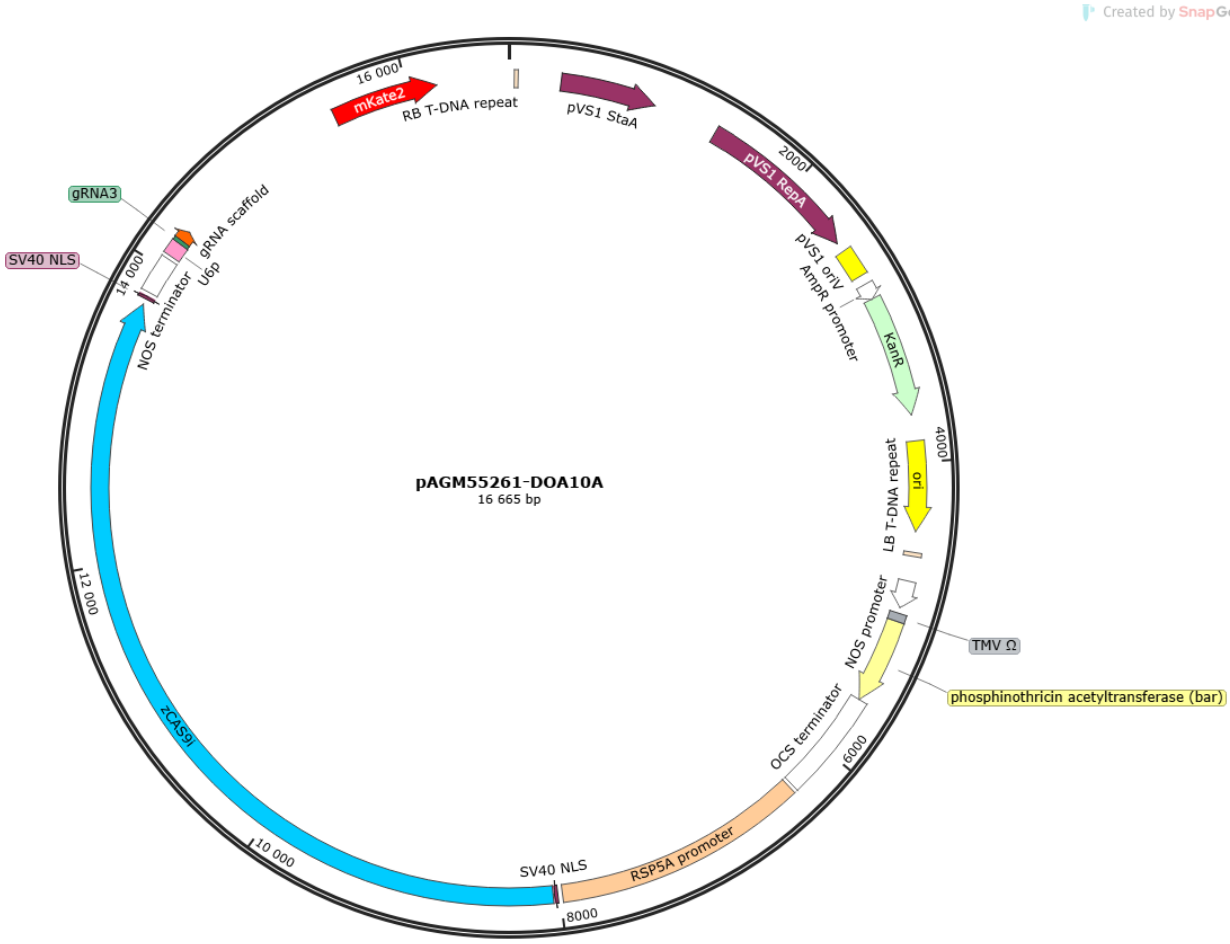

Figure 7. Plasmid map of the final pAGM55261-*DOA10A* construct (16,665 bp) generated in this study, showing the zCas9i expression cassette (pRPS5a promoter, SV40 NLS), the gRNA3 expression cassette (U6 promoter, gRNA scaffold), the *bar* selection cassette (phosphinothricin acetyltransferase), the FAST-associated mKate2 marker, and vector backbone elements (KanR, pVS1 origin, LB/RB T-DNA repeats). Map generated using SnapGene software.

3.4.3 Transformation into *Agrobacterium tumefaciens*

The verified pAGM55261-*DOA10A* CRISPR/Cas9 construct was introduced into *Agrobacterium tumefaciens* by electroporation. The cells were recovered in SOC medium for 2 h at 28 °C with shaking after transformation.

Recovered cells were plated on LB agar containing rifampicin, gentamicin and kanamycin and incubated at 28 °C for two days for selection of transformants.

Positive colonies were used to prepare Agrobacterium cultures for floral-dip transformation of *Arabidopsis* plants.

3.4.4 Floral-Dip Transformation and Selection

Floral-dip transformation was carried out as described by (Clough and Bent.,1998). A starter culture of Agrobacterium tumefaciens containing pAGM55261-*DOA10A* CRISPR/Cas9 construct was prepared in 250 mL liquid LB containing appropriate antibiotics and grown at 28 °C for 16 h. Agrobacterium cells were collected by centrifugation at 4000 × g for 10 min at room temperature.

Cell pellets were resuspended in freshly prepared infiltration solution consisting of 5% (w/v) sucrose. Silwet L-77 was added to a final concentration of 0.02% (v/v) immediately before just prior plant transformation and mixed thoroughly.

For floral-dip transformation, flowers of *Arabidopsis thaliana* plants at the flowering stage were flipped and dipped into Agrobacterium suspension. Plants were then held at room temperature for 24 h after treatment, and transferred back to standard growth conditions (22 °C, 16 h light / 8 h dark) for further development.

Because the recipient line already contained BASTA and kanamycin resistance markers, these could not be used for selection of transformants. Instead, the FAST marker system encoded within the pAGM55261 vector was intended to be used for seed-based screening of transgenic plants (Grützner et al., 2021). However, due to the end of the internship period, T_1 seeds were not yet harvested at the time of completion of the experimental work.

3.4.5 Selection of Cas9-Free Segregants

In a separate experiment, previously generated T_4 *doa10b*-3 sub-lines provided by the supervisor were used for segregation analysis and identification of putative Cas9-free individuals.

Seeds for analysis were from the *doa10b*-3 background (*pCKX3:CKX3-Venus ckx3 ckx5*; T_4 generation, line 5-3). The following sub-lines were included: 5-3-1, 5-3-8, 5-3-10, 5-3-12, and 5-3-13.

Seeds were surface sterilized and germinated on ½ Murashige and Skoog (½ MS) medium supplemented with hygromycin (25 µg mL^{-1}). Plates were incubated under controlled growth conditions (22 °C, 16 h light/8 h dark) for 7–10 days. Seedlings were scored for their response to hygromycin selection. Hygromycin-resistant seedlings were considered to carry the CRISPR/Cas9 T-DNA insertion, whereas hygromycin-sensitive seedlings were regarded as putative Cas9-free segregants.

To assess the presence of the Cas9 transgene, genomic DNA was isolated from selected seedlings and analyzed by PCR using the Cas9-specific primer pair 213 (forward) and 214 (reverse). PCR amplification products were separated by agarose gel electrophoresis and compared with those obtained from wild-type Col-0 controls. The PCR analysis was performed to distinguish transgene-positive from putative Cas9-free individuals.

Segregation patterns were recorded for each sub-line to assess inheritance of the CRISPR/Cas9 construct. Putative Cas9-free individuals were subsequently transferred to soil for further growth and downstream molecular analyses.

3.4.6 Genomic DNA Isolation and PCR Verification of Cas9 T-DNA

Genomic DNA was isolated from young leaves of *Arabidopsis thaliana* by SDS-based rapid extraction method as described in (Neff et al., 1998).

PCR-based genotyping was performed to verify the presence or absence of the CRISPR/Cas9 T-DNA insertion. Reactions were performed in 20 µL volumes with BioZtaq DNA polymerase and the provided 10x reaction buffer. Standard cycling conditions were used for the PCR amplification, with an annealing temperature of 53 °C and an extension time of 45 s.

Amplification products were separated by electrophoresis 1% agarose gel in 1× TAE buffer, stained with Midori Green Advance, and visualized using a gel

documentation system. Wild-type Col-0 and water controls were included as negative controls.

The presence or absence of the transgene was tested with primers 213 and 214, which amplify a ~600 bp fragment of the transgenic sgRNA scaffold region. Plants that had the expected amplification product were considered Cas9-positive, while those that did not show the expected band were considered putative Cas9-free segregants and were further genotyped if necessary to confirm their status.

3.5 Statistical Analysis

The effects of genotype, cytokinin treatment, and their interaction on root growth parameters were analyzed by two-way ANOVA followed by Tukey's post hoc test on data from the root growth assay.

Confocal microscopy data (TCSn::GFP fluorescence intensity) were analyzed using one-way ANOVA followed by Tukey's post hoc test to compare fluorescence intensity among genotypes.

Statistical analyses were performed using R software. Differences were considered statistically significant at $p < 0.05$. For each genotype, three biological replicates were analyzed.

4. Results

4.1 Genotyping of ERAD Mutants and TCSn::GFP Reporter Lines

4.1.1 PCR-based Genotyping

This experiment aimed to identify homozygous knockout plants for four ERAD components *HRD1A, HRD1B, DOA10A*, and *DOA10B*, within a background carrying the cytokinin reporter TCSn::GFP in *Arabidopsis thaliana*.

Segregating F_3-generation plants were analyzed from two independent lines: line 8 (8-1 to 8-20) and line 29 (29-1 to 29-4). The *DOA10A* allele was verified in these plants, while the remaining ERAD loci (*HRD1A, HRD1B, DOA10B*) were individually assessed through gene-specific and T-DNA–specific PCRs to determine their zygosity. For both T-DNA insertions and GFP amplification, wild-type Col-0 plants were used as negative controls. They amplified only gene-specific fragments, indicating correct primer function and absence of insertions.

PCR genotyping clearly distinguished wild-type, heterozygous and homozygous mutant alleles for each ERAD-related gene.

Representative gels for the *HRD1A* and *HRD1B* loci (Figures 8–12) showed good band resolution corresponding to wild-type (gene-specific) and mutant (T-DNA–specific) alleles.

PCR analysis of the twenty individuals from line 8 (8-1 to 8-20) revealed that individuals 8-1 and 8-4 were homozygous mutants for *HRD1B* because they only amplified the T-DNA-specific fragment while the gene-specific fragment was lacking. The amplification patterns of the other individuals on line 8 were consistent with either heterozygous or wild-type genotypes.

Individuals 8-1 and 8-4 did not carry the reporter transgene, according to PCR analysis of the TCSn::GFP reporter construct (Figure 12), since no GFP-specific amplification product was found.

The genotyping results enabled identification of plants with the desired ERAD mutant alleles and selection of individuals for subsequent analyses.

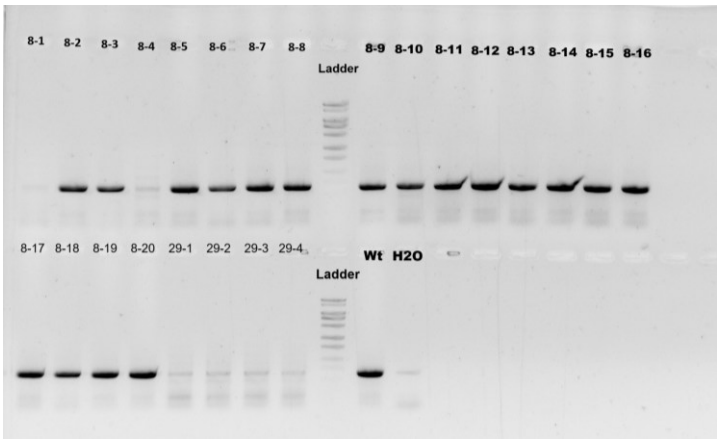

Figure 8. *HRD1B* locus PCR genotyping with gene-specific primers. Samples from lines 8 and 29 are shown using a 1 kb ladder; WT stands for wild type.

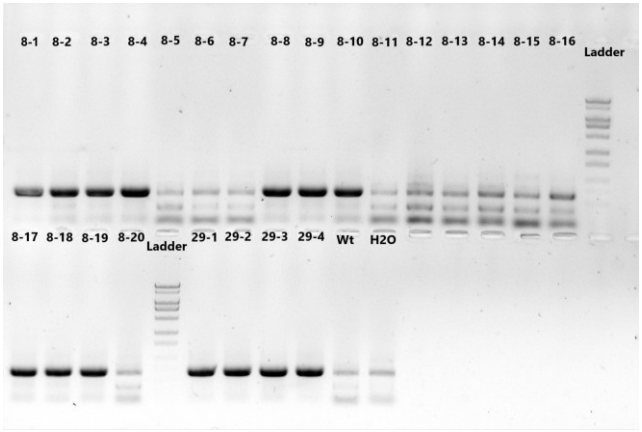

Figure 9. *HRD1B* locus PCR genotyping with T-DNA-specific primers. 1 kb ladder; WT: wild type; line 8 individuals 8-1 and 8-4 only display bands specific to insertions.

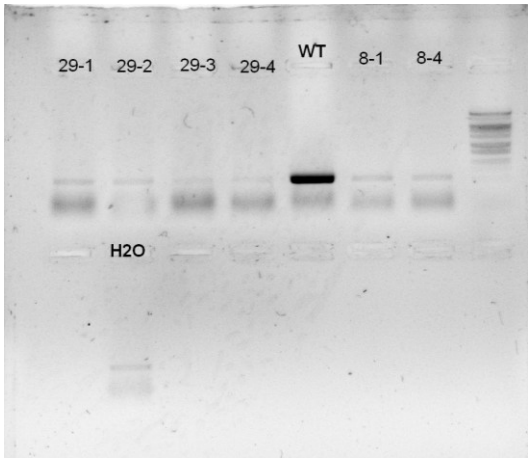

Figure 10. *HRD1A* locus PCR genotyping with gene-specific primers. WT: wild type; 1 kb ladder

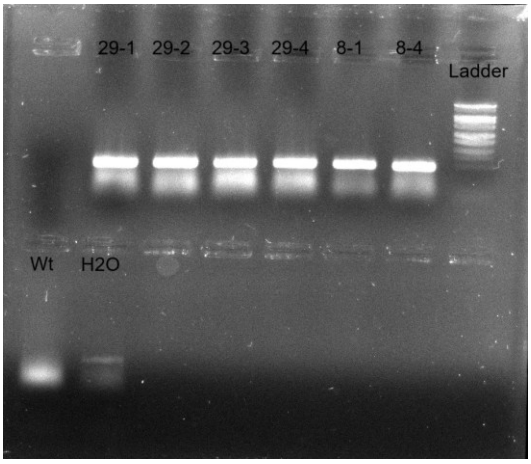

Figure 11. *HRD1A* locus PCR genotyping with T-DNA-specific primers. WT: wild type; 1 kb ladder.

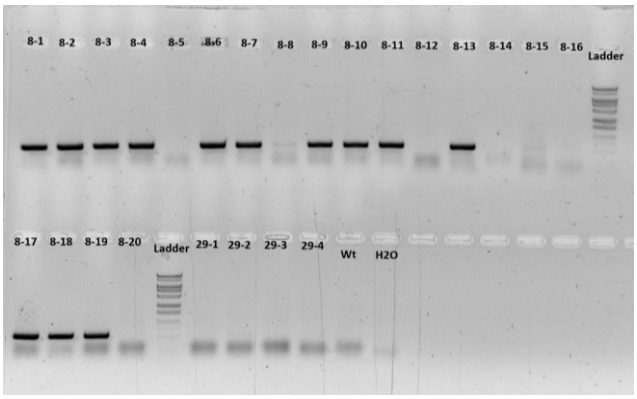

Figure 12. TCSn::GFP reporter construct amplification by PCR. 1 kb ladder.

4.1.2 Restriction Digest (CAPS Marker Analysis)

CAPS marker analysis was performed to determine the *DOA10A* and *DOA10B* genotypes of the selected plants (Figure 13). Following restriction enzyme digestion, wild-type Col-0 samples displayed the expected cleavage pattern, resulting in two DNA fragments. In contrast, samples 8-1, 8-4, and 29-1 to 29-4 showed a single undigested fragment, indicating the absence of the restriction site due to the respective point mutation.

No intermediate digestion pattern was observed in any sample. Since heterozygous individuals would be expected to display both digested and undigested fragments, the observed banding patterns indicate that all analyzed plants were homozygous for the mutant *DOA10A* and *DOA10B* alleles.

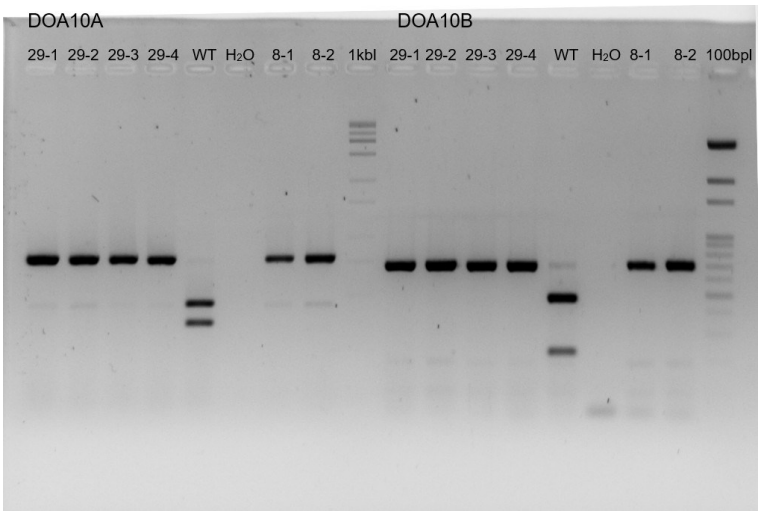

Figure 13. CAPS marker analysis of *DOA10A* and *DOA10B* alleles in *Arabidopsis thaliana*. Agarose gel electrophoresis was used to separate the PCR products that were amplified from the *DOA10A* and *DOA10B* loci after they had been digested with the appropriate restriction enzymes. Due to the lack of the restriction site, homozygous mutant samples revealed a single undigested fragment, while wild-type (WT) samples showed the expected digestion pattern with two fragments. The negative control was H2O. A 1 kb DNA ladder was used to assess fragment sizes.

4.2 Root assays

In order to assess the function of ER-associated degradation (ERAD) in cytokinin-dependent root development, we measured the length of the primary root (PR) and the number of lateral roots (LR) in wild-type *Arabidopsis thaliana* (Col-0) and the ERAD-deficient mutants *doa10a doa10b, hrd1a hrd1b*, and *hrd1a hrd1b doa10a doa10b*; The root growth responses of seedlings grown on media containing 0, 10, or 50 nM 6-benzylaminopurine (BA) were studied between genotypes and treatments.

4.2.1 Primary root length

Primary root (PR) length was strongly influenced by genotype, cytokinin treatment (BA), and their interaction (Figure 15); Cytokinin responses differed among genotypes based on hormone concentration, according to a two-way ANOVA that revealed significant effects of genotype ($p < 0.001$), BA concentration ($p < 0.001$), and a significant genotype × BA interaction ($p = 0.005$).

Small but sometimes significant differences in PR length were seen across genotypes under control conditions (Mock, 0 nM BA). In particular, the quadruple mutant (*hrd1a hrd1b doa10a doa10b*) had a slight but substantial increase in PR length (Figure 14) in comparison to Col-0 ($p < 0.01$), whereas the root length of the *hrd1a hrd1b* mutant was smaller than Col-0 ($p < 0.001$). There was no significant difference between Col-0 and *doa10a doa10b*. However these effects, that depended on the genotype, were relatively small when compared to the effect of cytokinin treatment.

At 10 nM BA, PR length was significantly reduced compared to control in Col-0 and the quadruple mutant ($p < 0.001$), and there was a modest but statistically significant reduction in *doa10a doa10b* ($p < 0.05$), despite the visual impression from the graph. In *hrd1a hrd1b*, the reduction in PR length at 10 nM BA compared to control was not statistically significant. At 50 nM BA, all genotypes displayed a strong and consistent inhibition of root length, resulting in similar PR length values (approximately 1.5–1.8 cm), and no significant differences were observed between genotypes at this concentration.

These results demonstrate that although genotype can influence primary root length under control conditions, cytokinin treatment is the dominant factor controlling root growth, resulting in strong and uniform inhibition across all lines at high BA concentrations (Figure 15).

4.2.2 Lateral root number

The number of lateral roots was significantly influenced by genotype, BA treatment, and their interaction; two-way ANOVA revealed significant effects of genotype ($p < 0.001$), BA concentration ($p < 0.0001$), and genotype x BA interaction ($p < 0.0001$), indicating genotype-dependent variations in cytokinin sensitivity.

Under control conditions, different genotypes had different numbers of lateral roots. While *hrd1a hrd1b* displayed decreased lateral root development, the *doa10a doa10b* double mutant displayed values close to Col. Under mock conditions, the quadruple mutant *hrd1a hrd1b doa10a doa10b* produced the most lateral roots.

At 10 nM BA, lateral root formation was significantly suppressed relative to control in all genotypes. Although the *doa10a doa10b* and quadruple mutants showed a visually higher mean number of lateral roots than Col-0 at this concentration, this difference did not reach statistical significance (Figure 16). At 50 nM BA lateral root formation was nearly completely inhibited in all genotypes and genotypic differences were greatly reduced.

In total, these results indicate that disruption of ERAD-related components alters cytokinin sensitivity during lateral root development and particularly at low BA concentrations (Figure 16).

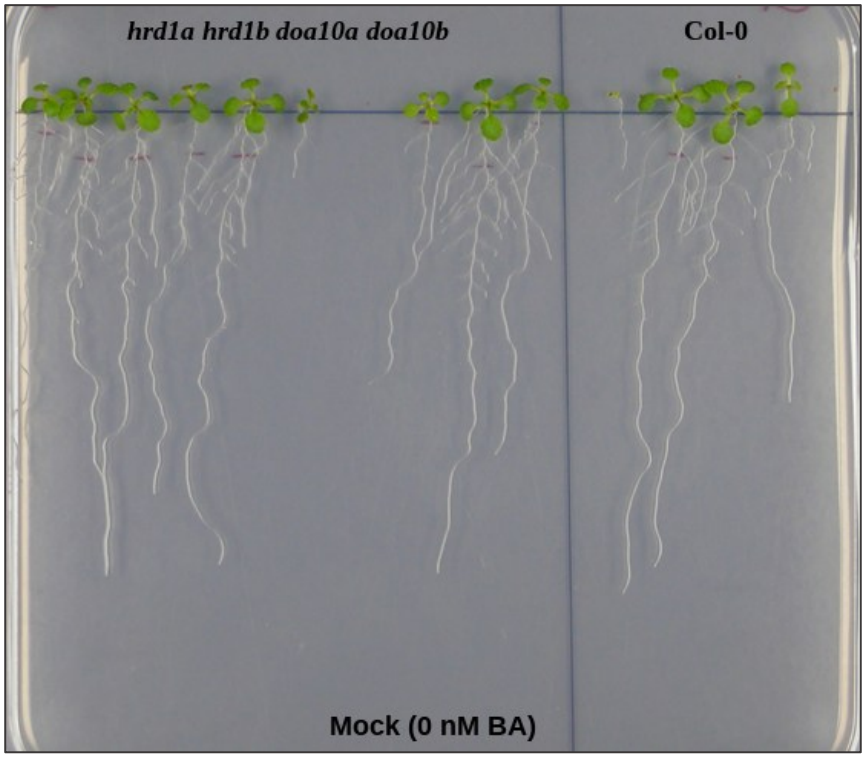

Figure 14. Representative root growth phenotype of Col-0 and the *hrd1a hrd1b doa10a doa10b* quadruple mutant under mock (0 nM BA) treatment, 6 days after transfer to light.

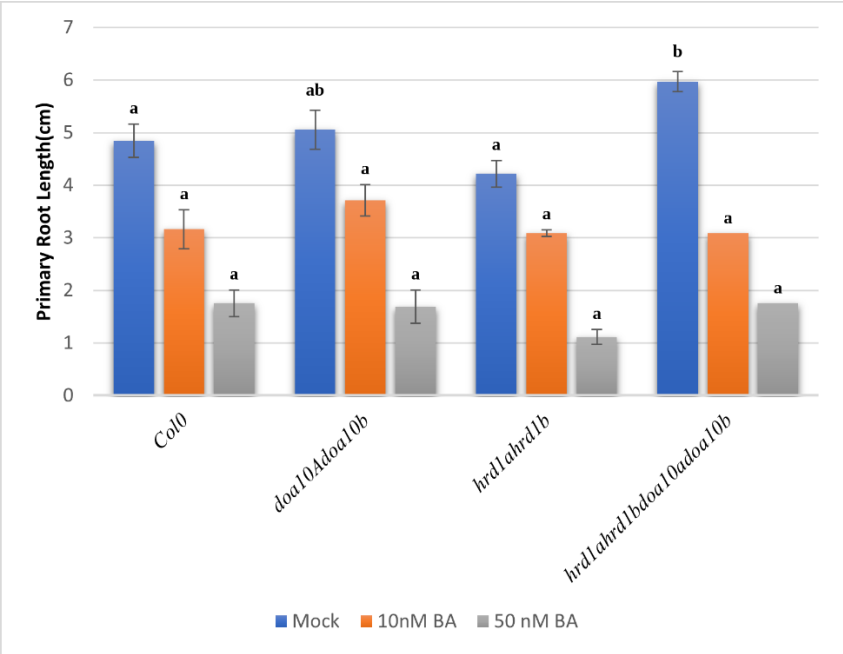

Figure 15. Primary root length in Col-0 and ERAD mutants under cytokinin treatment. Mean primary root length (± SE) for each genotype under mock (0 nM BA), 10 nM BA, and 50 nM BA treatment. Two-way ANOVA followed by Tukey's post hoc test; bars not sharing a letter differ significantly ($p < 0.05$) within each treatment.

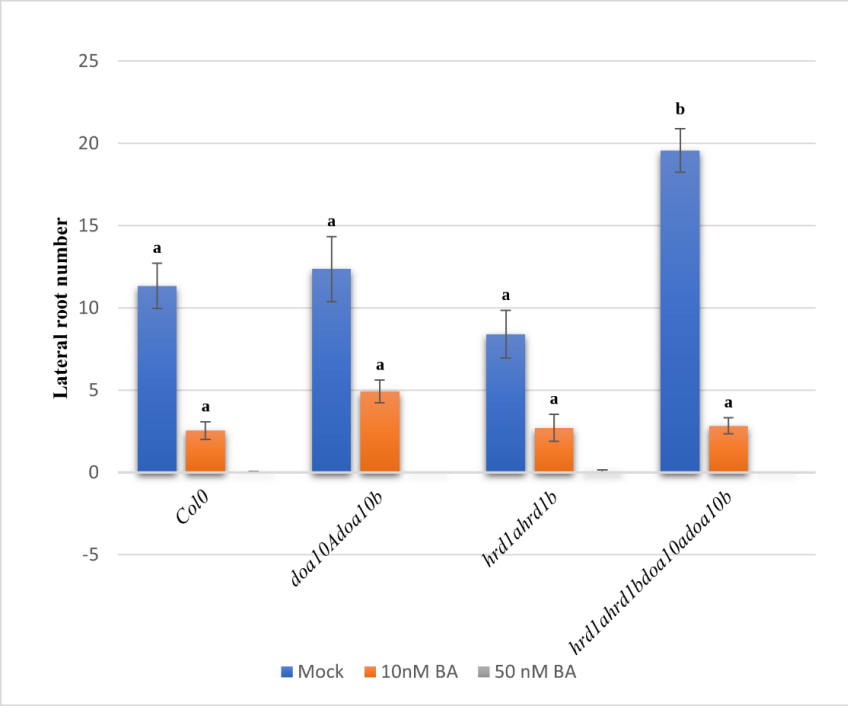

Figure 16. Lateral root number in Col-0 and ERAD mutants under cytokinin treatment. Mean lateral root number (± SE) for each genotype under mock (0 nM BA), 10 nM BA, and 50 nM BA treatment. Two-way ANOVA followed by Tukey's post hoc test; bars not sharing a letter differ significantly ($p < 0.05$) within each treatment. Lateral root formation was almost completely suppressed at 50 nM BA in all genotypes.

4.3 Confocal Analysis of TCSn::GFP Cytokinin Signaling in ERAD Mutants

This experiment investigated whether disruption of ER-associated degradation (ERAD) components affects cytokinin signaling output in the root cap of *Arabidopsis thaliana*, using the TCSn::GFP reporter line.

Quantification of GFP fluorescence revealed differences in cytokinin signalling activity depending on the genotype (Figure 17). The highest mean fluorescence intensity among the genotypes analyzed was observed in *doa10a* TCSn::GFP, while *hrd1a hrd1b* TCSn::GFP had the lowest mean fluorescence Intermediate levels of fluorescence were observed in the quadruple mutant (*hrd1a hrd1b doa10a doa10b* TCSn::GFP) and Col-0 TCSn::GFP.

GFP fluorescence intensity was significantly affected by the genotype in a one-way ANOVA ($F(3,75) = 5.19$, $p = 0.003$), which suggests that cytokinin signaling output was different between the genotypes studied.

According to Tukey's post hoc test, fluorescence intensity was substantially higher in *doa10a* TCSn::GFP than in *hrd1a hrd1b* TCSn::GFP ($p = 0.003$) and the quadruple mutant ($p = 0.037$). There were no additional statistically significant pairwise comparisons. Although *hrd1a hrd1b* TCSn::GFP showed less fluorescence than Col-0 TCSn::GFP, the difference was not statistically significant ($p = 0.076$).

Overall, our findings indicate that altered cytokinin signaling output in the root cap is related to disruption of specific ERAD components. The data show that TCSn::GFP reporter activity varies across the various genotypes of ERAD E3 ligase mutants.

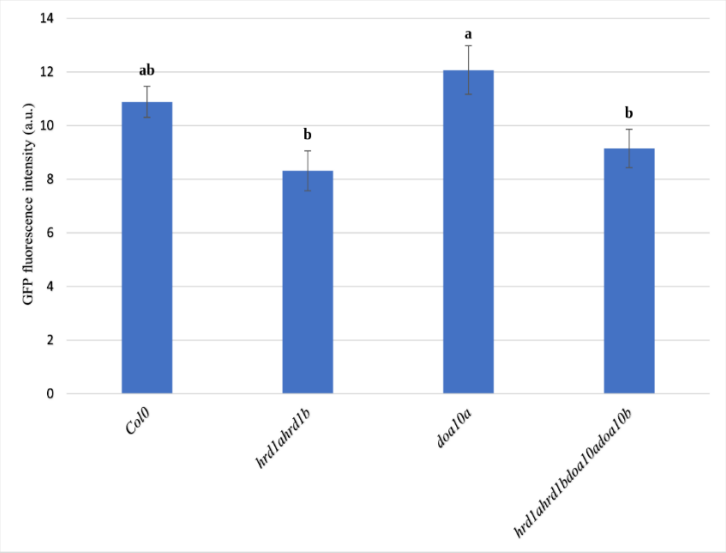

Figure 17. GFP fluorescence intensity in TCSn::GFP reporter lines across ERAD mutant backgrounds. Mean GFP fluorescence intensity (± SE) in the root cap for each genotype. One-way ANOVA followed by Tukey's post hoc test; bars not sharing a letter differ significantly ($p < 0.05$).

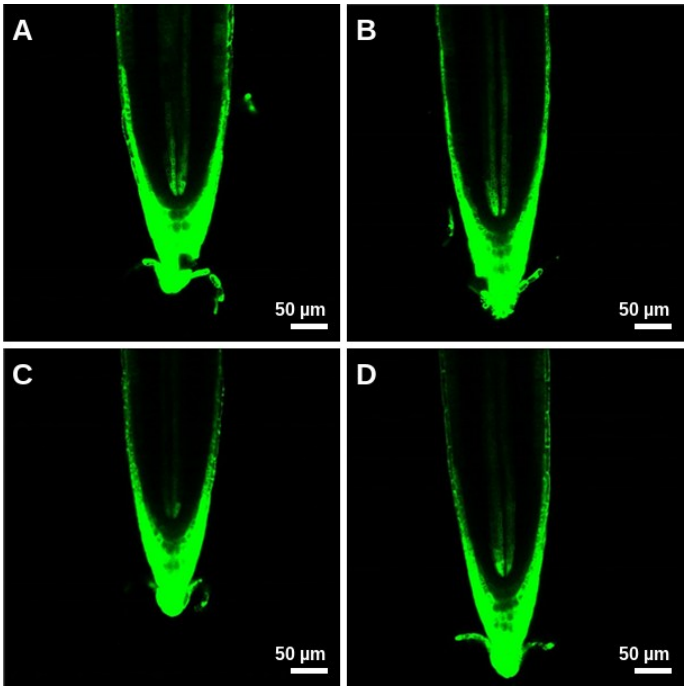

Figure 18. Representative confocal images of TCSn::GFP fluorescence in root cap cells. (A) Col-0, (B) *doa10a*, (C) *hrd1a hrd1b*, (D) *hrd1a hrd1b doa10a doa10b*.

4.4 Verification of the *DOA10A* CRISPR/Cas9 Construct

Clones containing the *DOA10A* sgRNA insert in the pAGM55261 CRISPR/Cas9 vector were identified by colony PCR screening of transformed Escherichia coli colonies. Using sgRNA-flanking primers, a particular amplification product of about 607 bp was found in positive colonies, indicating that the sgRNA construct had been successfully inserted (Figure 19).

Only colonies showing the expected PCR band were selected for further propagation and downstream applications.

Plasmid DNA was extracted from certain colonies and subjected to restriction enzyme digestion with NotI and NcoI in order to ensure correct assembly of the recombinant plasmid. The integrity of the pAGM55261-*DOA10A* CRISPR/Cas9

construct was confirmed by digestion, which yielded the anticipated fragment sizes of roughly 13.4 kb and 3.9 kb (Figure 20). After that, Agrobacterium tumefaciens was transformed using verified constructs.

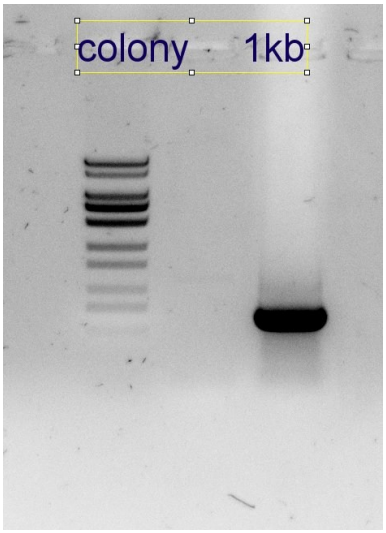

Figure 19. Colony PCR analysis of the pAGM55261-*DOA10A* CRISPR/Cas9 construct in transformed *E. coli* colonies. The expected amplification product of approximately 607 bp is demonstrated by positive colonies.

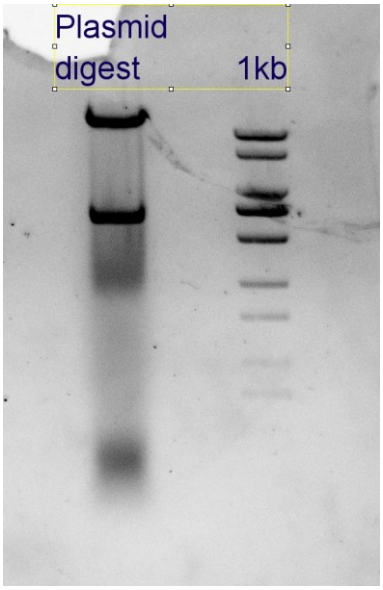

Figure 20. pAGM55261-*DOA10A* CRISPR/Cas9 plasmid restriction enzyme analysis based on NotI and NcoI digestion. The identified fragments matched the expected sizes of approximately 13.4 kb and 3.9 kb, confirming correct plasmid assembly.

4.5 Transformation and Selection of Transgenic Lines

Agrobacterium-mediated floral-dip transformation of *Arabidopsis thaliana* was performed using *Agrobacterium tumefaciens* strain GV3101 (pMP90) carrying the pAGM55261-*DOA10A* CRISPR/Cas9 construct; however, segregation analysis was conducted on previously generated T_4 lines derived from independent sub-lines of line 5-3 provided by the supervisor.

Transgenic seeds were obtained from independent lines derived from line 5-3. T-DNA insertion segregation was analyzed in sub-lines 5-3-1, 5-3-8, 5-3-10, 5-3-12, and 5-3-13.

In order to distinguish between transgene-positive and transgene-negative individuals, seedlings were grown on a medium containing hygromycin. All tested lines showed a distinct separation between hygromycin-sensitive and hygromycin-resistant seedlings. Sensitive seedlings displayed bleaching and growth inhibition under selection, while resistant seedlings showed normal development with green cotyledons and continued growth (Figure 21).

Hygromycin-resistant seedlings were considered to carry the CRISPR/Cas9 T-DNA insertion, whereas hygromycin-sensitive seedlings were selected for subsequent PCR-based screening to identify putative Cas9-free segregants.

Line	Hygromycin-resistant	Hygromycin-sensitive	No germination	Resistant : Sensitive
5-3-1	37	13	–	1:2.8
5-3-8	40	9	1	1:1.4
5-3-10	36	14	–	1:2.6
5-3-12	42	8	–	1:5.3
5-3-13	23	25	2	1:1

Table 5. Segregation analysis of hygromycin-resistant and hygromycin-sensitive seedlings in T-DNA insertion lines derived from line 5-3 sub-lines. Segregation ratios varied between sub-lines, indicating differences in T-DNA inheritance patterns across independent lines.

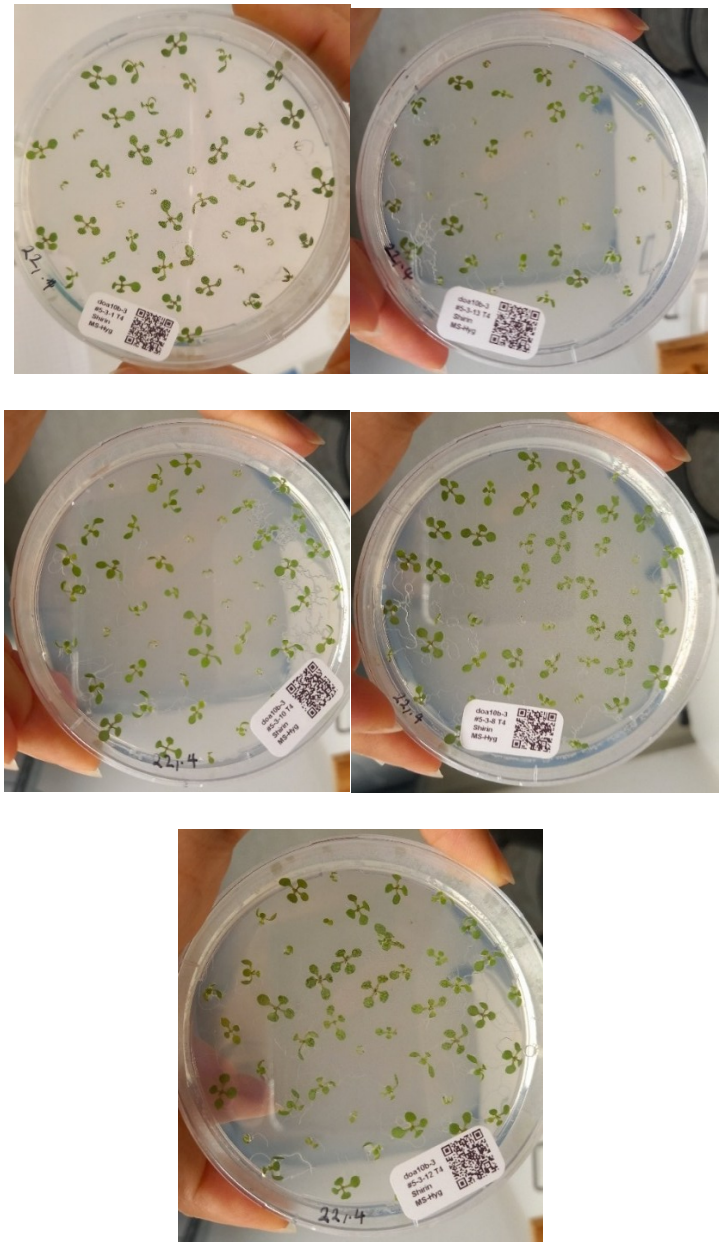

Figure 21. Representative T4 sub-lines showing segregation of hygromycin-resistant and hygromycin-sensitive seedlings. On selective medium resistant seedlings were green and grew normally while sensitive seedlings showed bleaching and inhibited growth.

4.5.1 Identification of Cas9-Free Segregants

PCR-based screening was performed to identify putative Cas9-free segregants among hygromycin-sensitive seedlings. Amplification using Cas9-specific primers produced bands in several analyzed samples; however, the banding pattern was not sufficiently clear to allow unambiguous discrimination between Cas9-positive and Cas9-negative individuals. Notably, amplification products were also detected in the wild-type control, which was expected to lack the CRISPR/Cas9 transgene. This indicated the presence of non-specific amplification under the PCR conditions used.

Due to the occurrence of bands in the wild-type control and the inconsistent amplification patterns observed among the tested samples, definitive identification of Cas9-free segregants could not be confirmed based on this PCR analysis alone. Therefore, the results were considered inconclusive and further optimization of primer specificity and PCR conditions would be required for reliable detection of transgene-free individuals.

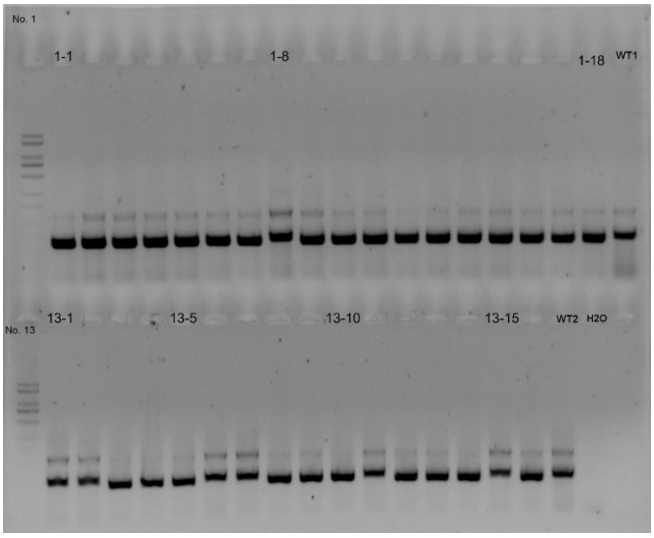

Figure 22. PCR-based screening of T_4 *Arabidopsis thaliana* seedlings using Cas9-specific primers 213 and 214. Amplification products were analyzed by agarose gel electrophoresis to assess the presence of the CRISPR/Cas9 transgene

5. Discussion

5.1 Genotyping of ERAD mutants and TCSn::GFP reporter lines

Accurate genotyping is a prerequisite for functional analyses of genetic mutants because reliable phenotypic and molecular characterization depends on the correct identification of mutant alleles. In this study, PCR-based genotyping combined with CAPS (cleaved amplified polymorphic sequence) marker analysis enabled reliable discrimination between wild-type, heterozygous, and homozygous alleles of the ERAD components. The agreement between PCR and CAPS analyses confirmed the genetic identity of the selected mutant lines and provided confidence for their use in subsequent experiments.

PCR screening also demonstrated that some plants carrying the desired ERAD mutant alleles lacked the TCSn::GFP reporter construct. Since the reporter is required for visualization of cytokinin-responsive gene expression, these plants were not suitable for confocal microscopy despite possessing the correct mutant genotype (Zürcher et al., 2013). This finding highlights the importance of verifying both mutant alleles and reporter transgenes when working with segregating populations, as inheritance of the mutation and the reporter construct occurs independently.

CAPS marker analysis further confirmed homozygosity of the *DOA10A* and *DOA10B* mutant alleles. The absence of heterozygous genotypes among the analyzed plants ensured that subsequent phenotypic analyses were performed using plants with complete loss of the targeted alleles, thereby reducing genetic variability that could complicate interpretation of the experimental results.

Overall, the combined genotyping strategy established a genetically defined set of experimental lines for the subsequent root growth and cytokinin signaling experiments. Careful validation of both the ERAD mutant alleles and the presence of the reporter construct strengthened the reliability of the phenotypic observations presented in this study.

5.2 Root assays

Root development is tightly regulated by phytohormones, with cytokinin acting as a key negative regulator of primary root elongation and lateral root formation (Kieber and Schaller, 2018). Cytokinin homeostasis is controlled by cytokinin oxidase/dehydrogenase (CKX) enzymes, which irreversibly degrade active cytokinins and thereby regulate their abundance within plant tissues (Werner et al., 2003; Sakakibara, 2006). Several CKX isoforms are localized to the endoplasmic reticulum, suggesting a potential functional connection with the ER-associated degradation (ERAD) pathway, which is responsible for maintaining protein quality by removing misfolded or damaged proteins from the ER (Hüttner and Strasser, 2012). Consequently, disruption of ERAD could affect cytokinin homeostasis through altered CKX protein turnover and thereby influence cytokinin-dependent root development. To investigate this possibility, the root growth responses of ERAD-deficient mutants to exogenous cytokinin were compared with those of wild-type plants.

Consistent with previous studies, exogenous cytokinin strongly inhibited primary root elongation in all genotypes. Cytokinin is known to restrict root meristem activity by reducing cell division and promoting the transition of meristematic cells into differentiation, thereby limiting root growth. Furthermore, cytokinin acts antagonistically to auxin within the root meristem, contributing to the regulation of root architecture (Kieber and Schaller, 2018). The pronounced reduction in primary root length following BA treatment therefore agrees well with the established role of cytokinin as a negative regulator of primary root development.

Although statistically significant differences in primary root length were observed between some genotypes under control conditions, these differences were relatively small compared with the effect of cytokinin treatment. This suggests that disruption of ERAD has only a limited influence on primary root development in the absence of hormonal stress. Rather than acting as a major determinant of root elongation, ERAD may contribute to the maintenance of protein homeostasis that supports normal cytokinin regulation. If ERAD participates in the quality control or turnover of ER-localized proteins involved in cytokinin homeostasis, including CKX

enzymes, impaired degradation could subtly alter cytokinin homeostasis without causing major developmental defects under standard growth conditions.

Interestingly, the *hrd1a hrd1b* mutant did not exhibit a statistically significant reduction in primary root length at 10 nM BA, whereas all other genotypes showed measurable cytokinin-mediated inhibition. This observation may indicate a modest alteration in cytokinin responsiveness at lower hormone concentrations. However, these differences disappeared at 50 nM BA, where all genotypes displayed similarly reduced primary root lengths. This finding suggests that high cytokinin concentrations produce a saturated inhibitory response that overrides relatively small differences in hormone sensitivity between genotypes. Therefore, the contribution of ERAD to primary root development appears to be relatively subtle and becomes detectable only under moderate cytokinin conditions.

Compared with primary root elongation, lateral root development appeared to be more strongly affected by disruption of ERAD components. Cytokinin is well known to suppress lateral root initiation by interfering with auxin transport and signaling, thereby restricting the formation of lateral root primordia (Laplaze et al., 2007; Kieber and Schaller, 2018). Consequently, changes in cytokinin homeostasis or signaling are often reflected more clearly in lateral root development than in primary root growth.

The observation that the *doa10a doa10b* double mutant, and particularly the *hrd1a hrd1b doa10a doa10b* quadruple mutant, showed a non-significant trend toward retaining more lateral roots following 10 nM BA treatment may hint at a partial reduction in cytokinin sensitivity, though this was not statistically confirmed in the present dataset and should be interpreted with caution. One possible explanation is that disruption of ERAD affects the stability or turnover of ER-localized proteins involved in cytokinin homeostasis, potentially including CKX proteins. Changes in CKX abundance or activity could alter cytokinin homeostasis, thereby reducing the inhibitory effect of BA on lateral root formation (Werner et al., 2003; Sakakibara, 2006). Alternatively, ERAD may influence the abundance or maturation of additional proteins involved in cytokinin perception or signaling. Because neither CKX protein accumulation nor cytokinin content was analysed in the present study,

these proposed mechanisms remain speculative and require experimental verification.

At the highest BA concentration, lateral root formation was almost completely suppressed in all genotypes and the differences between mutant lines and wild type were largely abolished. Similar to the primary root phenotype, this observation suggests that strong cytokinin treatment produces a maximal physiological response that masks relatively small effects caused by impaired ERAD function. Therefore, ERAD appears to contribute to the fine-tuning of cytokinin responses rather than determining the overall capacity of cytokinin to inhibit root development.

Overall, the root assays demonstrate that cytokinin is the dominant regulator of both primary root elongation and lateral root formation, whereas disruption of ERAD components produces comparatively subtle but reproducible effects on cytokinin responsiveness. The more pronounced phenotype observed during lateral root development suggests that this developmental process is particularly sensitive to changes in cytokinin homeostasis. Although the present results are consistent with the hypothesis that ERAD contributes to cytokinin regulation through effects on CKX protein homeostasis, direct evidence for this mechanism is still lacking. Future studies investigating CKX protein stability, cytokinin accumulation, and the turnover of ER-localized cytokinin-related proteins will be necessary to clarify the molecular basis underlying the altered root phenotypes observed in the ERAD mutants.

5.3 Confocal analysis of cytokinin signaling

Cytokinin responses in plants are mediated through a multistep signaling pathway that ultimately regulates transcriptional activity in target tissues. The synthetic TCSn::GFP reporter provides a sensitive readout of cytokinin signaling output and has been widely used to visualize spatial and quantitative changes in cytokinin responses at the cellular level (Zürcher et al., 2013). In this study, TCSn::GFP fluorescence was used to assess whether disruption of ER-associated degradation

(ERAD) components affects cytokinin signaling activity in the root cap of *Arabidopsis thaliana.*

The results show that cytokinin signaling output, as reflected by GFP fluorescence intensity, differs between ERAD mutant backgrounds. In particular, the *doa10a* mutant exhibited significantly higher TCSn::GFP activity compared with both the *hrd1a hrd1b* double mutant and the quadruple mutant. This indicates that disruption of specific ERAD components can lead to altered cytokinin signaling output at the tissue level. The presence of statistically significant differences between genotypes supports the conclusion that ERAD function is linked to the regulation of cytokinin responsiveness in the root cap.

Interestingly, the *hrd1a hrd1b* double mutant showed a tendency toward reduced TCSn::GFP fluorescence compared with wild type, although this difference was not statistically significant. This suggests that loss of *HRD1* function alone may have a weaker or more variable effect on cytokinin signaling compared with *DOA10* disruption. The strongest effect observed in the *doa10a* line may indicate that *DOA10*-dependent ERAD pathways play a more prominent role in maintaining proper cytokinin signaling output than *HRD1*-dependent pathways, at least in the root cap tissue analyzed here.

The intermediate fluorescence levels observed in the quadruple mutant further suggest that simultaneous disruption of multiple ERAD branches does not necessarily produce an additive effect on cytokinin signaling output. One possible explanation is that redundancy and compensation between ERAD pathways may limit the overall impact of combined mutations. Alternatively, severe disruption of ER protein quality control could trigger compensatory stress responses that indirectly influence hormone signaling pathways, thereby buffering the expected additive effect.

From a physiological perspective, the observed differences in TCSn::GFP activity suggest that ERAD contributes to the fine-tuning of cytokinin signaling intensity rather than determining whether signaling occurs at all. This is consistent with the root growth phenotypes, where ERAD mutants showed altered sensitivity to

cytokinin rather than a complete loss of response. Together, these findings support the idea that ERAD influences cytokinin signaling indirectly, most plausibly through its effect on the turnover of ER-localized components such as CKX, rather than by acting directly within the phosphorelay itself.

One possible mechanistic explanation is that ERAD affects the stability or turnover of proteins involved in cytokinin perception or signaling, such as ER-localized cytokinin receptors or other ER-associated regulatory components. Cytokinin signaling has been proposed to originate predominantly from the endoplasmic reticulum, highlighting the ER as an important site for cytokinin perception and signal transduction (Romanov et al., 2018). Consequently, disruption of ER protein quality control could indirectly influence cytokinin signaling output. Alternatively, changes in cytokinin signaling may arise through altered cytokinin homeostasis, for example via effects on cytokinin oxidase/dehydrogenase (CKX) proteins, which regulate cytokinin degradation and overall cytokinin levels within plant tissues (Werner et al., 2003; Sakakibara, 2006). However, because neither receptor abundance, CKX protein levels, nor endogenous cytokinin concentrations were analysed in this study, the precise molecular mechanism underlying the altered TCSn::GFP activity remains unresolved.

Overall, the confocal analysis demonstrates that disruption of ERAD components leads to measurable changes in cytokinin signaling output in the root cap. Although the effects vary between different ERAD mutants, the results consistently indicate that ERAD contributes to the modulation of cytokinin responsiveness at the tissue level. This supports the broader conclusion of this study that ER protein quality control plays a regulatory role in hormone-dependent root development.

5.4 Verification of the *DOA10A* CRISPR/Cas9 construct and selection of transgenic lines

Successful construction of the CRISPR/Cas9 vector represents a critical prerequisite for downstream genome editing experiments, as incorrect assembly would compromise all subsequent transformation steps (Feng et al., 2013). In this

study, colony PCR and restriction enzyme digestion provided complementary validation of the pAGM55261-*DOA10A* construct. The detection of the expected sgRNA-specific PCR product confirmed correct insertion of the guide RNA cassette, while restriction analysis further verified correct plasmid assembly based on the anticipated fragment sizes. Together, these results indicate that the CRISPR/Cas9 construct was properly assembled and suitable for *Agrobacterium*-mediated plant transformation.

Following plasmid verification, transformation into *Agrobacterium tumefaciens* and subsequent floral-dip transformation of *Arabidopsis thaliana* enabled the generation of transgenic seed material, a widely used and efficient method for stable plant transformation (Clough and Bent, 1998). Segregation analysis of independent T_4 sub-lines derived from line 5-3 revealed variation in the ratio of hygromycin-resistant to hygromycin-sensitive seedlings. While some lines approximated the expected Mendelian segregation patterns for a single T-DNA insertion, others showed deviations from the ideal 3:1 ratio. Such variation is commonly observed in transgenic plant populations and may reflect differences in T-DNA insertion number, insertion site effects, or partial silencing of the selection marker.

The clear phenotypic distinction between hygromycin-resistant and hygromycin-sensitive seedlings confirmed the effectiveness of the selection system, allowing reliable discrimination between transgene-positive and transgene-negative individuals. Resistant seedlings were therefore considered to carry the CRISPR/Cas9 T-DNA, whereas hygromycin-sensitive seedlings provided a valuable source for identifying Cas9-free segregants in subsequent PCR-based screening. The identification of Cas9-free lines is particularly important because it enables stable analysis of edited plants after segregation of the CRISPR/Cas9 transgene, thereby preventing continued Cas9 activity in later generations.

Overall, the combined molecular verification of the CRISPR/Cas9 construct and phenotypic segregation analysis established a well-characterized experimental population for subsequent genetic screening and mutant identification.

6. Conclusion

This study aimed to investigate whether disruption of core ER-associated degradation (ERAD) components — *HRD1A/HRD1B* and *DOA10A/DOA10B* — affects cytokinin-regulated root development in *Arabidopsis thaliana*, building on the previously established link between ERAD and CKX turnover (Guo et al., 2021).

Regarding primary root growth and lateral root formation (Research Question 1), genotype had a statistically significant but comparatively modest effect relative to the dominant influence of exogenous cytokinin. Under control conditions, the *hrd1a hrd1b doa10a doa10b* quadruple mutant displayed a longer primary root and a greater number of lateral roots than Col-0, while *hrd1a hrd1b* showed the opposite trend. These genotype-dependent differences were largely masked at higher cytokinin concentrations, where all lines converged on a strongly suppressed root phenotype.

Regarding cytokinin signaling output (Research Question 2), TCSn::GFP fluorescence in the root cap differed significantly between genotypes, with *doa10a* showing significantly higher signaling activity than both *hrd1a hrd1b* and the quadruple mutant. No other pairwise comparisons reached statistical significance.

Regarding whether these findings point to a cytokinin-deficiency-like or cytokinin-overaccumulation-like state (Research Question 3), the results do not support a single, uniform direction across all ERAD branches. The enhanced root growth observed in the quadruple mutant under control conditions is more consistent with a cytokinin-deficiency-like phenotype, whereas the elevated TCSn::GFP signal in *doa10a* points toward locally increased signaling in that background specifically. This apparent discrepancy suggests that *HRD1*- and *DOA10*-dependent ERAD branches may not contribute equivalently to cytokinin regulation, and that combined disruption of both branches does not produce a simple additive effect — potentially reflecting redundancy, compensation, or branch-specific substrate preferences within the ERAD pathway.

Taken together, these findings indicate that ERAD contributes to the fine-tuning of cytokinin sensitivity in root tissues rather than acting as a core, obligatory component of cytokinin signaling or root development. Because CKX protein abundance, CKX enzymatic activity, and endogenous cytokinin levels were not directly measured in this study, the precise molecular mechanism linking ERAD disruption to the observed phenotypes remains undetermined. Future work directly assessing CKX protein stability and activity, together with cytokinin quantification in the relevant ERAD mutant backgrounds, will be necessary to distinguish between the possible mechanisms proposed here and to clarify the specific contribution of *HRD1*- versus *DOA10*-dependent ERAD branches to cytokinin homeostasis in the root.

References

Aloni, R., Langhans, M., Aloni, E., & Ullrich, C. I. (2006). Role of cytokinin and auxin in shaping root architecture: Regulating vascular differentiation, lateral root initiation, root apical dominance and root gravitropism. *Annals of Botany, 97*(5), 883–893. https://doi.org/10.1093/aob/mcl027

Argyros, R. D., Mathews, D. E., Chiang, Y.-H., Palmer, C. M., Thibault, D. M., Etheridge, N., Argyros, D. A., Mason, M. G., Kieber, J. J., & Schaller, G. E. (2008). Type-B response regulators of *Arabidopsis* play key roles in cytokinin signaling and plant development. *The Plant Cell, 20*(8), 2102–2116. https://doi.org/10.1105/tpc.108.059584

Benfey, P. N., & Scheres, B. (2000). Root development. *Current Biology, 10*(22), R813–R815. https://doi.org/10.1016/S0960-9822(00)00814-9

Bishopp A, Help H, El-Showk S, et al. (2011) A mutually inhibitory interaction between auxin and cytokinin specifies vascular pattern in roots. *Current Biology* 21:917–926. https://doi.org/10.1016/j.cub.2011.04.017

Bürkle, L., Cedzich, A., Döpke, C., Stransky, H., Okumoto, S., Gillissen, B., Kühn, C., & Frommer, W. B. (2003). Transport of cytokinins mediated by purine transporters of the PUP family expressed in phloem, hydathodes, and pollen of *Arabidopsis*. *The Plant Journal, 34*(1), 13–26. https://doi.org/10.1046/j.1365-313X.2003.01700.x

Caesar, K., Thamm, A. M. K., Witthöft, J., Elgass, K., Huppenberger, P., Grefen, C., Horak, J., & Harter, K. (2011). Evidence for the localization of the *Arabidopsis* cytokinin receptors AHK3 and AHK4 in the endoplasmic reticulum. *Journal of Experimental Botany, 62*(15), 5571–5580. https://doi.org/10.1093/jxb/err236

Chang, L., Ramireddy, E., & Schmülling, T. (2015). Cytokinin as a positional cue regulating lateral root spacing in *Arabidopsis*. *Journal of Experimental Botany, 66*(15), 4759–4768. https://doi.org/10.1093/jxb/erv252

Christianson, J. C., & Ye, Y. (2014). Cleaning up in the endoplasmic reticulum: Ubiquitin in charge. *Nature Structural & Molecular Biology, 21*(4), 325–335. https://doi.org/10.1038/nsmb.2796

Clough, S. J., & Bent, A. F. (1998). Floral dip: A simplified method for Agrobacterium-mediated transformation of *Arabidopsis* thaliana. *The Plant Journal, 16*(6), 735–743. https://doi.org/10.1046/j.1365-313x.1998.00343.x

Dello Ioio, R., Linhares, F. S., Scacchi, E., Casamitjana-Martinez, E., Heidstra, R., Costantino, P., & Sabatini, S. (2007). Cytokinins determine *Arabidopsis* root-meristem size by controlling cell differentiation. *Current Biology, 17*(8), 678–682. https://doi.org/10.1016/j.cub.2007.02.047

Dolan, L., Janmaat, K., Willemsen, V., Linstead, P., Poethig, S., Roberts, K., & Scheres, B. (1993). Cellular organisation of the *Arabidopsis* thaliana root. *Development, 119*(1), 71–84. https://doi.org/10.1242/dev.119.1.71

Feng, Z., Zhang, B., Ding, W., Liu, X., Yang, D.-L., Wei, P., Cao, F., Zhu, S., Zhang, F., Mao, Y., & Zhu, J.-K. (2013). Efficient genome editing in plants using a CRISPR/Cas system. *Cell Research, 23*(10), 1229–1232. https://doi.org/10.1038/cr.2013.114

Grützner, R., Martin, P., Horn, C., Mortensen, S., Cram, E. J., Lee-Parsons, C. W. T., Stuttmann, J., & Marillonnet, S. (2021). High-efficiency genome editing in plants mediated by a Cas9 gene containing multiple introns. *Plant Communications, 2*(1), 100135. https://doi.org/10.1016/j.xplc.2020.100135

Guo, T., Weber, H., Niemann, M. C. E., Theisl, L., Leonte, G., Novák, O., & Werner, T. (2021). *Arabidopsis* HIPP proteins regulate endoplasmic reticulum-associated degradation of CKX proteins and cytokinin responses. *Molecular Plant, 14*(11), 1918–1934. https://doi.org/10.1016/j.molp.2021.07.015

Hirose, N., Takei, K., Kuroha, T., Kamada-Nobusada, T., Hayashi, H., & Sakakibara, H. (2008). Regulation of cytokinin biosynthesis, compartmentalization and translocation. *Journal of Experimental Botany, 59*(1), 75–83. https://doi.org/10.1093/jxb/erm157

Hutchison CE, Li J, Argyros RD, et al. (2006) The *Arabidopsis* histidine phosphotransfer proteins are redundant positive regulators of cytokinin signaling. *Plant Cell* 18:3073–3087. https://doi.org/10.1105/tpc.106.045674

Hüttner, S., & Strasser, R. (2012). Endoplasmic reticulum-associated degradation of glycoproteins in plants. *Frontiers in Plant Science, 3*, Article 67. https://doi.org/10.3389/fpls.2012.00067

Hwang, I., Sheen, J., & Müller, B. (2012). Cytokinin signaling networks. *Annual Review of Plant Biology, 63*, 353–380. https://doi.org/10.1146/annurev-arplant-042811-105503

Kieber, J. J., & Schaller, G. E. (2014). Cytokinins. *The Arabidopsis Book, 12*, e0168. https://doi.org/10.1199/tab.0168

Kieber, J. J., & Schaller, G. E. (2018). Cytokinin signaling in plant development. *Development, 145*(4), dev149344. https://doi.org/10.1242/dev.149344

Ko, D., Kang, J., Kiba, T., Park, J., Kojima, M., Do, J., Kim, K. Y., Kwon, M., Endler, A., Song, W.-Y., Martinoia, E., Sakakibara, H., & Lee, Y. (2014). *Arabidopsis* ABCG14 is essential for the root-to-shoot translocation of cytokinin. *Proceedings of the National Academy of Sciences, 111*(19), 7150–7155. https://doi.org/10.1073/pnas.1321519111

Kurakawa, T., Ueda, N., Maekawa, M., Kobayashi, K., Kojima, M., Nagato, Y., Sakakibara, H., & Kyozuka, J. (2007). Direct control of shoot meristem activity by a cytokinin-activating enzyme. *Nature, 445*(7128), 652–655. https://doi.org/10.1038/nature05504

Kuroha, T., Tokunaga, H., Kojima, M., Ueda, N., Ishida, T., Nagawa, S., Fukuda, H., Sugimoto, K., & Sakakibara, H. (2009). Functional analyses of LONELY GUY cytokinin-activating enzymes reveal the importance of the direct activation pathway in *Arabidopsis*. *The Plant Cell, 21*(10), 3152–3169. https://doi.org/10.1105/tpc.109.068676

Laplaze, L., Benková, E., Casimiro, I., Maes, L., Vanneste, S., Swarup, R., Weijers, D., Calvo, V., Parizot, B., Herrera-Rodriguez, M. B., Offringa, R., Graham, N., Doumas, P., Friml, J., Bogusz, D., Beeckman, T., & Bennett, M. (2007). Cytokinins act directly on lateral root founder cells to inhibit root initiation. *The Plant Cell, 19*(12), 3889–3900. https://doi.org/10.1105/tpc.107.055863

Lei, Y., Lu, L., Liu, H.-Y., Li, S., Xing, F., & Chen, L.-L. (2014). CRISPR-P: A web tool for synthetic single-guide RNA design of CRISPR-system in plants. *Molecular Plant, 7*(9), 1494–1496. https://doi.org/10.1093/mp/ssu044

Lin, L., Zhang, C., Chen, Y., Wang, Y., Wang, D., Liu, X., Wang, M., Mao, J., Zhang, J., Xing, W., Liu, L., & Li, J. (2019). PAWH1 and PAWH2 are plant-specific components of an *Arabidopsis* endoplasmic reticulum-associated degradation complex. *Nature Communications, 10*, 3492. https://doi.org/10.1038/s41467-019-11480-7

Liu, J.-X., & Howell, S. H. (2016). Managing the protein folding demands in the endoplasmic reticulum of plants. *New Phytologist, 211*(2), 418–428. https://doi.org/10.1111/nph.13915

Malamy, J. E., & Benfey, P. N. (1997). Organization and cell differentiation in lateral roots of *Arabidopsis* thaliana. *Development, 124*(1), 33–44. https://doi.org/10.1242/dev.124.1.33

Miyawaki, K., Tarkowski, P., Matsumoto-Kitano, M., Kato, T., Sato, S., Tarkowska, D., Sandberg, G., & Kakimoto, T. (2006). Roles of *Arabidopsis* ATP/ADP isopentenyltransferases and tRNA isopentenyltransferases in cytokinin biosynthesis. *Proceedings of the National Academy of Sciences, 103*(44), 16598–16603. https://doi.org/10.1073/pnas.0603522103

Mok, D. W. S., & Mok, M. C. (2001). Cytokinin metabolism and action. *Annual Review of Plant Physiology and Plant Molecular Biology, 52*, 89–118. https://doi.org/10.1146/annurev.arplant.52.1.89

Müller, B., & Sheen, J. (2008). Cytokinin and auxin interaction in root stem-cell specification during early embryogenesis. *Nature, 453*(7198), 1094–1097. https://doi.org/10.1038/nature06943

Murashige, T., & Skoog, F. (1962). A revised medium for rapid growth and bio assays with tobacco tissue cultures. *Physiologia Plantarum, 15*(3), 473–497. https://doi.org/10.1111/j.1399-3054.1962.tb08052.x

Neff, M. M., Neff, J. D., Chory, J., & Pepper, A. E. (1998). dCAPS, a simple technique for the genetic analysis of single nucleotide polymorphisms: Experimental applications in *Arabidopsis* thaliana genetics. *The Plant Journal, 14*(3), 387–392. https://doi.org/10.1046/j.1365-313x.1998.00124.x

Niemann, M. C. E., Weber, H., Hluska, T., Leonte, G., Anderson, S. M., Novák, O., Senes, A., & Werner, T. (2018). The cytokinin oxidase/dehydrogenase CKX1 is a membrane-bound protein requiring homooligomerization in the endoplasmic reticulum for its cellular activity. *Plant Physiology, 176*(3), 2024–2039. https://doi.org/10.1104/pp.17.00925

Péret, B., Larrieu, A., & Bennett, M. J. (2009). Lateral root emergence: A difficult birth. *Journal of Experimental Botany, 60*(13), 3637–3643. https://doi.org/10.1093/jxb/erp232

Romanov, G. A., Lomin, S. N., & Schmülling, T. (2018). Cytokinin signaling: From the ER or from the PM? That is the question! *New Phytologist, 218*(1), 41–53. https://doi.org/10.1111/nph.14991

Ruzicka K, Simásková M, Duclercq J, et al. (2009) Cytokinin regulates root meristem activity via modulation of auxin transport. *PNAS* 106(11):4284-9. https://doi.org/10.1073/pnas.0900060106

Sakakibara, H. (2006). Cytokinins: Activity, biosynthesis, and translocation. *Annual Review of Plant Biology, 57*, 431–449. https://doi.org/10.1146/annurev.arplant.57.032905.105231

Scheres, B., & Benfey, P. N. (2002). Root development. *The Arabidopsis Book, 1*, e0101. https://doi.org/10.1199/tab.0101

Schindelin, J., Arganda-Carreras, I., Frise, E., Kaynig, V., Longair, M., Pietzsch, T., Preibisch, S., Rueden, C., Saalfeld, S., Schmid, B., Tinevez, J.-Y., White, D. J., Hartenstein, V., Eliceiri, K., Tomancak, P., & Cardona, A. (2012). Fiji: An open-source platform for biological-image analysis. *Nature Methods, 9*(7), 676–682. https://doi.org/10.1038/nmeth.2019

Schmülling, T., Werner, T., Riefler, M., Krupková, E., & Bartrina y Manns, I. (2003). Structure and function of cytokinin oxidase/dehydrogenase genes of maize, rice, *Arabidopsis* and other species. *Journal of Plant Research, 116*(3), 241–252. https://doi.org/10.1007/s10265-003-0096-4

Shimada, T. L., Shimada, T., & Hara-Nishimura, I. (2010). A rapid and non-destructive screenable marker, FAST, for identifying transformed seeds of *Arabidopsis thaliana*. *The Plant Journal, 61*(3), 519–528. https://doi.org/10.1111/j.1365-313X.2009.04060.x

Strasser, R. (2018). Protein quality control in the endoplasmic reticulum of plants. *Annual Review of Plant Biology, 69*, 147–172. https://doi.org/10.1146/annurev-arplant-042817-040331

To JP, Haberer G, Ferreira FJ, et al. (2004) Type-A *Arabidopsis* response regulators are partially redundant negative regulators of cytokinin signaling. *Plant Cell* 16(3):658–671. https://doi.org/10.1105/tpc.018978

Werner, T., Köllmer, I., Bartrina, I., Holst, K., & Schmülling, T. (2006). New insights into the biology of cytokinin degradation. *Plant Biology, 8*(3), 371–381. https://doi.org/10.1055/s-2006-923928

Werner, T., Nehnevajova, E., Köllmer, I., Novák, O., Strnad, M., Krämer, U., & Schmülling, T. (2010). Root-specific reduction of cytokinin causes enhanced root growth, drought tolerance, and leaf mineral enrichment in *Arabidopsis* and tobacco. *The Plant Cell, 22*(12), 3905–3920. https://doi.org/10.1105/tpc.109.072694

Werner, T., Motyka, V., Laucou, V., Smets, R., Van Onckelen, H., & Schmülling, T. (2003). Cytokinin-deficient transgenic *Arabidopsis* plants show multiple developmental alterations indicating opposite functions of cytokinins in the regulation of shoot and root meristem activity. *The Plant Cell, 15*(11), 2532–2550. https://doi.org/10.1105/tpc.014928

Werner, T., & Schmülling, T. (2009). Cytokinin action in plant development. *Current Opinion in Plant Biology, 12*(5), 527–538. https://doi.org/10.1016/j.pbi.2009.07.002

Wu, J., Huang, P., & Li, J. (2026). The *Hrd1*-mediated ERAD pathway in plants: Conserved principles and plant-specific innovations. *International Journal of Molecular Sciences, 27*(4), 1801. https://doi.org/10.3390/ijms27041801

Wulfetange, K., Lomin, S. N., Romanov, G. A., Stolz, A., Heyl, A., & Schmülling, T. (2011). The cytokinin receptors of *Arabidopsis* are located mainly to the endoplasmic reticulum. *Plant Physiology, 156*(4), 1808–1818. https://doi.org/10.1104/pp.111.180539

Zhao, J., Wang, J., Liu, J., Kudoyarova, G., Liu, C.-J., & Zhang, K. (2024). Spatially distributed cytokinins: Metabolism, signaling, and transport. *Plant Communications, 5*(8), 100936. https://doi.org/10.1016/j.xplc.2024.100936

Zürcher, E., Liu, J., Di Donato, M., Geisler, M., & Müller, B. (2016). Plant development regulated by cytokinin sinks. *Science, 353*(6303), 1027–1030. https://doi.org/10.1126/science.aaf7254

Zürcher, E., Tavor-Deslex, D., Lituiev, D., Enkerli, K., Tarr, P. T., & Müller, B. (2013). A robust and sensitive synthetic sensor to monitor the transcriptional output of the cytokinin signaling network in planta. *Plant Physiology, 161*(3), 1066–1075. https://doi.org/10.1104/pp.112.211763